ACP Discussions: acpd-15-9941-2015
(Editor - Federico Fierli)
'Impact of different Asian source regions on the composition of the Asian monsoon anticyclone and on the extratropical lowermost stratosphere'

We thank both referees for their comments and their willingness to read the manuscript once again. We added the useful technical suggestions. Following the editor's advice we prepared a letter of response for reviewer 1 criticisms (see below). Our reply to the reviewer #1 and #2 comments is listed in detail below. Questions and comments of the referees are shown in italics.

Author Comment to Referee #1

The revision is an improvement over the original manuscript and is close to being publishable. There are many grammatical errors and confusing passages as well as an overabundance hyperbole and misleading statements. There are three sections that contain too much description of unnecessary and uninteresting details, two of these (Sec. 3.1 [up to Sec. 3.1.1] and 3.2 [up to Sec. 3.2.1) should be condensed (Sec. 3.1 could easily be summarized in a paragraph) and the third (last two paragraphs of Sec. 3.1.2) could be deleted along with Fig. 6. The most serious and important criticism is that the manuscript ignores (or barely acknowledges) how the design of the CLaMS experiments affect the interpretation of the results.

We thank reviewer #1 for the technical comments. Before the paper will be finalised, the ACP production department and the language service at Forschungszentrum Jülich will check the manuscript to make sure that the quality of the English of the paper is satisfactory. We think that to understand the behaviour of the Asian monsoon anticyclone 2012 it is important to describe its temporal variability in Sect. 3.1 and 3.2. In response to the reviewer comment, Section 3.2 is somewhat shortened. To our knowledge there is no other publication in which such a detailed description of the temporal variability of the Asian monsoon at tropopause heights is included. Of course we acknowledge that there is a vast literature on the variability of monsoon patterns at lower tropopause heights. Therefore we are convinced that it is an interesting and important information for the reader to understand our results concerning the temporal variability of the composition of the Asian monsoon anticyclone in 2012.

1. *The first of these criticisms concerns potential weaknesses of CLaMS. Transport models, such as CLaMS, have many weaknesses that affect scientific results; these models depend on reliable data to initialize constituent concentrations, reliable wind data to properly transport air parcels, and process models to alter constituents along parcel pathways. A major problem with CLaMS is its dependence on resolved winds from ERA-interim to simulate convective transport. It is possible to mitigate the impact of these weaknesses with careful analysis (for example, through time and ensemble averaging), but they cannot be simply ignored as is the case in this paper. What is particularly troubling about this paper is the statement (line 8, page 13) that suggests that deficiencies in MLS CO data could lead to the disagreement between CLaMS and MLS. There is no doubt that observational error contributes to the disagreement, but to ignore the impact of model error and, therefore, imply that only observational error is at fault is worse than misleading. The authors must discuss how model weaknesses might be affecting their results.*

The reviewer points correctly to a problem that all transport and trajectory models have in principle, namely they have to rely on the accuracy of the meteorological fields from (re)analysis. We accept that differences between MLS CO and CLaMS could also be caused by deficiencies of the model. However, the accuracy of CLaMS transport of CO in convective situations was tested to a considerable extend against in-situ measurements (Pommrich et al., 2014). Further, deficiencies of MLS CO were also noted by Schwartz et al. (2015) (no cited in the revised version). We revised the paragraph related to MLS measurements in Sect. 3.1.1 as follows:

‘Correlation coefficients of 0.57 to 0.81 were calculated for both MLS(CO)/ CLaMS(CO) and MLS(CO)/CLaMS(India/China) between end of June and end of September. These high correlation coefficients confirm that CLaMS has the capability of simulating the spatial distribution of tropospheric trace gases such as CO and stratospheric trace gases like O_3 measured by MLS. In the region of the Asian monsoon anticyclone, the correlation coefficients of MLS(O_3)/CLaMS(O_3) are somewhat higher than those of MLS(CO)/ CLaMS(CO). Reasons for this observation could be deficiencies in MLS

CO data (v3) in the lower stratosphere as found by Schwartz et al. (2015), who detect a lack of expected signatures in MLS (v3) CO in the context of double tropopauses e. g. on the poleward edge of the Asian monsoon anticyclone and suggest that these deficiencies could be related to unexpectedly weak equator-to-pole gradients of MLS CO in the lower stratosphere (Hegglin and Tegtmeier, 2015). Differences between MLS(CO)/CLaMS(CO) and MLS(O_3)/CLaMS(O_3) correlations could also be caused by limitations in the convective transport of CO in ERA-Interim reanalysis data (see discussion in Sect. 4) or by lower boundary conditions for CO (see Sect. 2.1).'

The dependence of CLaMS results on resolved winds from ERA-interim data is discussed in more detail in the context of the following point below.

2. *The second criticism concerns an issue I mentioned in my original review, that the authors have addressed, but not with enough substance. The issues concerns the ability of CLaMS to faithfully represent regional tracer concentrations (Fig. 8) in the anticyclone during summer when those tracers were initialized only after May 1st while transport times from the boundary layer to the 380 K isentrope can exceed 90 days. The problem is nicely demonstrated in Fig. 3 of the response to review #1 (which should be included in the manuscript) in which it is shown that the boundary layer contribution to air in the anti-cyclone does not exceed 50% until early August. That, however, is only part of the problem. Boundary layer air from different regions have different transport times. So, this 'spin-up' problem (as I called it in my previous review) affects different regions differently – so that the relative contributions from different regions are not faithfully represented in Fig. 8. In the revision, the authors do mention the fact that regional tracer concentrations do not account for air parcels in the boundary layer before May 1 and they do acknowledge that it takes time for concentrations of boundary layer tracer to build up, but that is not enough. They must explicitly acknowledge that this phenomenon affects the interpretation of their results and, if possible, discuss how it affects their results. If this was my work, I would perform an additional CLaMS experiment that starts 3 months earlier to see if the results change form the May 1 experiment and I would examine boundary layer to 380 K transport times from the different regions – regions with longer transport times will be more affected by model initialization.*

Following the reviewers advice we added the new Fig. 1 (= Fig. 3 of the response to review #1) and added the following discussion section to the manuscript in Sect. 4. Further, while we accept this point for additional CLaMS runs (but for a future study) we argue that in our study we address a different question then that addressed by additional model runs initialised 3 months earlier. Here, we focus on the upward transport during one particular monsoon season, therefore the model runs is initialised just before the monsoon season 2012.:

'In this paper, we want to show how the impact of different emission tracers changes during the course of the Asian monsoon season 2012 with the focus on the influence of fresh emissions from different regions. Therefore, we selected 1 May 2012 as the start point for our simulation which is before the formation of the Asian monsoon anticyclone. Of course, air masses emitted in the Earth's boundary layer before 1 May 2012 will contribute to the composition of the Asian monsoon anticyclone, however here we aim at quantifying the impact of young air masses in one particular Asian monsoon season that experienced upward transport in the vicinity of the Asian monsoon anticyclone. Our results therefore demonstrate the influence of young air masses on the composition of the Asian monsoon and on the extratropical lowermost stratosphere. Using this approach we could show that on the end of the monsoon season in September up to 75 % of the air masses within the Asian monsoon anticyclone are younger than 5 months (see Fig. 1). That implies that the impact of air masses older than 5 months has only a moderate impacts on the composition of the Asian monsoon anticyclone at the end of the monsoon season. Our results demonstrate that the Asian monsoon system is an effective pathway for transport of air masses from the Earth's surface into the upper troposphere within a few months during the course of the Asian monsoon season 2012.
In contrast to our study, Orbe et al. (2015) used tracers of air mass origin in model simulations to infer the impact of boundary regions in Asia to the tropical lower stratosphere with an approach that the different tracers have equilibrated so that the sum of all tracers of air mass origin is equal to unity within the entire atmosphere (using a spin-up of 20 years). This approach provides for each air parcel the information about the origin within the boundary layer. However, this approach provides no information on the transport times from the boundary layer in Asia to the tropical lower stratosphere. To infer the transport times in the approach by Orbe et al. (2015), they introduce a boundary impulse response that marks air that left the

boundary layer on a certain day (1 July). They infer transport times of one month from the boundary layer in Asia into the tropical lower stratosphere in July when the Asian monsoon is active. In this respect, their pulse serves a similar purpose as our seasonal tracer setup. However, our approach considers all air masses that left the boundary layer over the course of the monsoon season 2012 since May and thus reflects so the meteorological conditions of the entire monsoon season 2012.

In our approach, the absolute percentages of the emission tracers found within the Asian monsoon anticyclone depend on the start point of the model simulations on 1 May 2012. However, the temporal behaviour of the individual emission tracers depends on convective processes causing strong upward transport within the Asian monsoon anticyclone in summer 2012 and are therefore a fingerprint of the regional and temporal variations during the course of the monsoon season. This approach gives insights in the temporal variability of the composition of the Asian monsoon anticyclone over the course of the monsoon period 2012 in addition to earlier studies which analysed the origin of air masses within the Asian monsoon anticyclone for a certain shorter period of the monsoon season (e. g. Li et al., 2005; Bergman et al., 2013) or infer mean values of air mass origin for the entire monsoon season (e. g. Park et al., 2009; Chen et al., 2012; Fadnavis et al., 2014).

The upward transport and convection in CLaMS is driven by ERA-Interim reanalysis data in which changes are implemented to improve deep and mid-level convection compared to previous reanalysis data (Dee et al., 2011). However, small-scale rapid uplift in convective cores is not included. We expect that in data sets additionally including the small-scale rapid uplift in convective cores, the uplift of air masses within the Asian monsoon should be even more pronounced. However, previous studies (e. g. Ploeger et al., 2010; Pommrich et al., 2014; Vogel et al., 2014) show that ERA-Interim reanalysis data are well suited to study transport processes in the vicinity of the Asian monsoon anticyclone and in the tropical tropopause layer (TTL). In addition, in CLaMS the diabatic approach with potential temperature as the vertical coordinate (Pommrich et al., 2014) is used which is suggested to yield more reliable results compared to kinematic calculations (e. g. Ploeger et al., 2010; Bergman et al., 2015).'

To perform an additional simulation that starts 3 months earlier to see if the results change from a simulation that starts on 1 May is certainly a good suggestion. However, it would prolong the transport times that are considered within our model experiment. If we did such a simulation we would

also include upward transport of air masses before the monsoon season in winter/spring 2012. This issue is also interesting to examine, but would answer a different question. Our work answers the question what is the impact of different boundary layer source regions in Asia on the composition of the Asian monsoon anticyclone during the course of one particular monsoon season. Therefore only fresh emissions or young air masses are considered.
Taking up the idea of reviewer #1, we will perform a new study (which is beyond the scope of this paper) implementing an age spectrum for each emission tracer to answer the question about the transport times of different emission regions. That would also include the upward transport of air masses before the monsoon season that contribute to the composition of the Asian monsoon anticyclone.

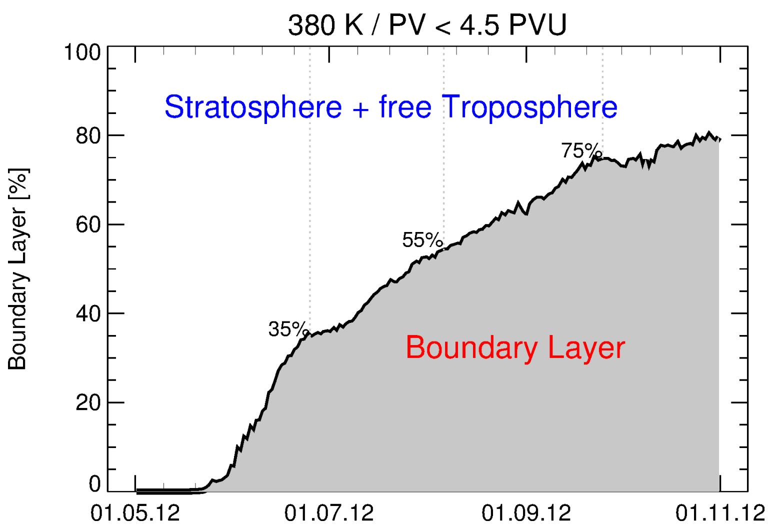

Figure 1: Temporal evolution of contributions of air masses from the boundary layer to the composition of the Asian monsoon anticyclone. The shown percentages are mean values calculated for air masses in Asia in the region between 15 and 50 N and 0 and 140 E at 380 ± 0.5 K (see black rectangle in Fig. 7) with PV values lower than 4.5 PVU that marks the edge of the anticyclone.

Specific comments:

Note, the line numbers are messed up on my copy of the manuscript. I used the number as marked until the numbers on the manuscript reset to 0. At that point I continue using numbers that are not reset. For example, the last line on page 17 is labeled number 5 – I count that as line number 34.

Page 2, lines 16-17: Remove the clause 'and is therefore more complex than hitherto believed'. One would have to be ignorant of atmospheric research from the past 50 years to not believe dynamics of the anti-cyclone to be this complex.

This statement (and this has now been clarified) refers to the behaviour of the Asian monsoon anticyclone at upper tropospheric altitudes. To our knowledge there are no publications that, for upper tropospheric altitudes, have analysed the impact of different Asian source regions on the composition of the Asian monsoon anticyclone depending on time over the course of an entire monsoon season. Therefore, here we think it is warranted to use this statement, in this way.

P.2 L.21-23: Remove the sentence 'Our findings ... the Asian monsoon anticyclone.' This is a trivial result. Also 'memorized' is not grammatically correct in this context. 'Imprinted' or 'recorded' would be grammatically correct.

done

P.2 L.24-27: The sentence 'Air masses ... of the anticyclone' should be rephrased. It is awkward and confusing.

done

P.6 L.9,11,14: Change 'Sect.' to 'Sec.'

In ACP publications use of 'Sect.' is enforced.

P.7 l.29-30: Reword the phrase 'tracer-tracer correlations were used similarly as for the initialisation besides CO'. Its meaning is unclear.

done

P.8 L.5: Regarding the sentence 'Water vapour is replaced by ECMWF water vapour in lower model levels'. I assume you mean that you use ECWMF water vapor for lower levels because satellites do not observe those levels. Regardless, rephrase to make it clear what you mean.

done

P.8 L.11: Remove 'further the'.

done

P.8 L.15: Remove 'to quantify'.

done

Sec. 3.1 [P. 9 L.24 to P.12 L.7]: This section contains a lot of description of unnecessary details. Please consider replacing most of the content with a single, to the point, paragraph.

To our knowledge there is no other publication in which such a description of the temporal variability of the Asian monsoon anticyclone is included. Therefore we think that is an interesting and important information to the reader.

P.9 L.10-11: Regarding 'At each time step of the model (every 24 hours)'. The CLaMS model time step can't possibly be 24 h (probably closer to 20 min).

revised to: 'Every 24 hours (time step for mixing in CLaMS) air masses in the model boundary layer are marked by the different emission tracers ...'

P.10 L18: Replace 'here' with 'when'.

done

P.10 L.20: The sentence 'On 12 September 2012 conditions during the late-phase of the monsoon and on 7 October 2012 the situation after the breakup of the anticyclone occurring end-September are shown' is awkward and seemingly has no important content.

done

P.10 L.23-25: Rephrase the sentence 'The northern ... equatorial easterly jet'.

We are not sure why. Please note that the paper will be copy edited.

P.12 L.21-22: Regarding the phrase 'are normalised so that the maximum value of each trace gas is equal one'. You can delete this phrase. It is not necessary to normalize by the maximum value; the correlation calculation does its own normalization (by the standard deviation – after the mean is removed).

We do not agree with this critique. The normalisation to one is necessary to calculate the correlation coefficient between the spatial distribution of artificial tracers and chemical species.

P. 13 L.4: Regarding 'These high correlations'. What constitutes a high correlation depends on context. Here, since the fields are supposed to be identical – the correlations should be 1.0. The model data only explains 50-65% of the observed variability. It would benefit you to examine correlations between weekly or monthly averages to see how the correlation is affected by data sampling.

Caused by deficits in both model and measurements (e. g. spatial resolution) it is not to be expected to get correlation coefficients of one or even close to one. As described in Sect. 3.1, there is a strong temporal variability of the shape and location of the Asian monsoon anticyclone. Therefore, in our calculation of pattern correlation coefficients the variability of the Asian monsoon anticyclone from day to day is considered.

P.13 L.8: Regarding 'Reasons for that could be deficiencies in MLS CO'. Please do not place all of the blame for the disagreement on observational *error. If you mention problems with the observational data, then you must also mention problems with the model (which are substantial and their impact on your results should be acknowledged whether or not you mention observational error).*

We agree; see above point 1.

P. 13 L.14 and L.16: 'A remarkable good correlation' and 'a very good proxy' are both overstatements (two examples of the hyperbole mentioned above). Statements regarding the utility of the model as a proxy should be confined to those that help the reader understand which aspects are well represented by the model, which aspects are not, and why. In this context 'very good' is not specific enough and, therefore, meaningless. Also, while the correlations are important, whether or not a proxy is good can only be tested using predictions (e.g., via linear regression) and how good those predictions are depends on the context. There is no context given in this manuscript from which to judge the quality of the proxy.

We agree with the first point and 'remarkable' is removed. The expression 'proxy' is used here in the following sense: 'In statistics, a proxy or proxy variable is a variable that is not in itself directly relevant, but that serves in place of an unobservable or immeasurable variable. In order for a variable to be a good proxy, it must have a strong correlation with the variable of interest.' Because the pattern correlation between the emission tracer for India/China is strongly correlated to the pattern of MLS CO and strongly anticorrelated to MLS O_3 and PV, the spatial distribution of emission tracer for India/China is by definition a good proxy for the spatial distribution of the Asian monsoon anticyclone.

P. 13 L.22: Change 'the the' to 'to the'.

done

P.13 L.26: Remove 'also'.

done

P.13 L.26: Change 'correlation' to 'correlations'.

done

P.13 L.31: Change 'similar as for' to 'similar to' or 'as were'.

done

P.14 L.11: Change 'increases' to 'increase'.

done

P.14 L.13: The wording of 'the missing convection in Asia occurring during' is awkward. Suggestion: 'the lack of convection in Asia during'

done

P.14 L.28: 'very good proxy' is an over statement – both that statement and 'good correlation' are meaningless without a well-defined context.

done

P.14. L.26 – P.15 L.20: I would remove these paragraphs and Fig. 6. They contribute nothing meaningful to the paper.

Fig. 6 demonstrates the local shift of the Asian monsoon depending on time. The local shift of the Asian monsoon is connected to variation in the composition of tracers of air mass origin within the Asian monsoon anticyclone as explained in the paper. Therefore we did not remove Fig. 6.

Sec. 3.2 [P. 15 L.23 to P.18 L.25]: This section contains too much description of unnecessary details. Please condense.

done

P.15 L.28: Improper use of 'in principle'. Consider a change of wording such as 'show primarily the same ...' or 'primarily show the same ...' of 'show, in general, the same ...'

done

P. 16 L.12: Change 'are in addition found' to 'are also found'.

done

P. 16 L.15: Change 'in the same order' to 'of the same order'.

done

P.16 L.17-19: Change 'Similar as for 1 July 2012, on 2 August 2012 in the mid-phase at 380 K (Fig. 7, 2nd row, left) the distribution of the emission tracer for North India is also confined within the Asian monsoon anticyclone' to 'Similar to distributions on 1 July 2012, the distribution of the emission tracer for North India on 2 August 2012 in the mid-phase at 380 K (Fig. 7, 2nd row, left) is also confined within the Asian monsoon anticyclone'.

done

P.16 L.20-21: Change 'Contrary to the 1 July at the beginning of August, the highest percentages of emission tracers within the anticyclone are ...' to 'In contrast to 1 July, the highest percentages of emission tracers within the anticyclone at the beginning of August are ...'

done

P. 16 L.29: Change 'Sect.' to 'Sec.'

In ACP publications use of 'Sect.' is enforced.

P.17 L.7 (actually, the first line): change 'having large contributions' to 'which have large contributions'

done

P.17 L. 27: Change 'parcel' to 'parcels'.

done

P.17 L.29: Change 'evident in the strong gradients' to 'as evident in the strong gradients' or 'as evidenced by the strong gradients'.

done

P.17 last line: Change 'A subsequently isentropic' to 'The subsequent isentropic'.

done

P.18 L.22: The use of 'flooded' is great imagery, is provocative, and has stylist power. Unfortunately it is another example of hyperbole. Please change it.

We agree with the reviewer that the use of 'flooded' has stylist power. However, Figure 7 shows that on 12 September in the entire northern hemisphere contributions from Southeast Asia between 6-10% are found. Therefore, we think the expression 'flooded' is warranted.

P.19 L.21: Change 'tracer' to 'tracers'.

done

P.20 L.11: Change 'In principle' to 'In general'.

done

P.21 L.7 (second line): Change 'However then' to 'However, when'.

done

P.21 L.14: Change 'Sect.' to 'Sec.'

In ACP publications use of 'Sect.' is enforced.

P.21 L.12-23: This paragraph might work better at the beginning of the Section.

done

P.21 L.24-33: This paragraph should be replaced with a discussion that explicitly acknowledges that the initial condition of this experiment (i.e., starting on May 1) might affect the results. I recommend the following: include Fig. 3 from the response to Review #1, an additional CLaMS experiment that is initialized earlier in the year (e.g., Feb. 1), and calculate transport times for the different regional tracers as a way to estimate the impact of initial conditions on the results.

See above point 2.

P.22 L11-12: Remove 'remarkable'

done

P.22 L.18-21: Remove the sentence 'The good agreement ... Asian monsoon anticyclone'. Your work does not predict values of PV using tracer distributions and so you do not provide enough proof nor define a context in which to claim that tracers are a good proxy. Furthermore, you don't use those distributions as a proxy, which makes the statement unnecessary.

see above definition of proxy

P.22 L25-27: Change 'After the breakup of the anticyclone in early-October, still high percentages for the emission tracer for India/China are located over India, China and the Pacific Ocean' to 'High percentages for the emission tracer for India/China located over India, China and the Pacific Ocean are still found after the breakup of the anticyclone in early October'.

done

P.22 L.28: Change 'In this paper, we could answer the question of what is the impact of different boundary layer sources in Asia to the Asian monsoon anticyclone in summer 2012' to 'In this paper, we address the question: what is the impact of different boundary layer sources in Asia to the Asian monsoon anticyclone in summer 2012?'

Here, we would like to emphasise the 'answer' not the 'question', therefore the statement is formulated as answer and not as question like in the introduction.

P.22 L.31: Change 'have an impact on the composition of the Asian monsoon anticyclone in contrast to all' to 'have a larger impact on the composition of the Asian monsoon anticyclone than all'.

done

P.23 L.22: The statement 'Therefore the processes are more complex than hitherto believed' does not follow logically from the previous statements and, furthermore, is undoubtedly wrong. Please remove it.

The sentence is revised as follows: 'The variability of the composition of the Asian monsoon anticyclone over the course of the monsoon season is therefore more complex than hitherto believed.'
P.24 L.8 (first line): Change 'flooding'

see above

Author Comment to Referee #2

The revised version of the manuscript has very much improved compared to the original version. The authors have followed my advice to remove parts from the manuscript. This makes the new manuscript much clearer, more focused and easier to follow. Further, comparison to observations and analysis of the model data have been significantly improved by putting them on a broader statistical basis. I recommend publishing of the manuscript after a few very minor, possibly even only technical corrections:

Minor/technical comments:

Page 5, l22/23: what is "normal"? I think you mean that the monsoon conditions were not extreme in any way. Another wording like "medium" ore "average" would be more appropriate.

done

Page 6, l7: you had two questions on page 6, l17-21, therefore change "question" to "questionS".

reformulated to one question

Page 11, l 30ff (subtropical jet as transport barrier): How do you identify the subtropical jet? Where do you see it in the figures? And what about the "blob" near 60N, 150W in Fig.3, lower panels? I think this argument needs some re-working.

The sentence is revised as follows: 'High percentages of the emission tracers for India/China are found over the Pacific Ocean and over the east coast of North America along the subtropical westerly jet and in filaments separated at the northeastern flank from the Asian monsoon anticyclone (Vogel et al., 2014).'

Page 12, l3: Is the transport into the UPPER stratosphere really relevant in this context, or do you just want to say that the air is transported further up into the stratosphere?

We agree. The sentence is revised as follows: 'In addition, air masses originating in the boundary layer in India/China could penetrate into the upwelling in the deep branch of the Brewer–Dobson circulation and thus could be transported further up into the stratosphere.'

Page 12, l30/31: Is there an explanation that the correlation between MLS and CLaMS is even better before formation of the anticyclone? Strictly speaking your finding means that either MLS or CLaMS or both have difficulties representing the anticyclone properly, while they do much better for monsoon-free conditions. Any comment on this?

The sentence is revised as follows: 'Before the monsoon season in early May an even higher correlation coefficient up to 0.95 was found for MLS(O_3)/ CLaMS(O_3) most likely caused by the fact that the initial O_3 fields in CLaMS for 1 May 2012 are derived from MLS data (see 2.1).'

Page 13, l8/9: What exactly are the deficiencies identified for CO from MLS? If the data are just biased, this should not affect your correlation analysis. For an impact on the correlation analysis, the data would need to have a higher scatter, or any systematic errors related to specific atmospheric situations that are different in the anticyclone than outside, like temperature or the pressure level. The reference to an unpublished manuscript is not sufficient in my opinion at this place here. Please provide either another reference accessible at the time of publication of your manuscript or explain in more detail what the identified problems with MLS were.

We agree that more discussion of MLS CO data is required here. We revised this paragraph as follows:

'Correlation coefficients of 0.57 to 0.81 were calculated for both MLS(CO)/ CLaMS(CO) and MLS(CO)/CLaMS(India/China) between end of June and end of September. These high correlation coefficients confirm that CLaMS has the capability of simulating the spatial distribution of tropospheric trace gases such as CO and stratospheric trace gases like O_3 measured by MLS. In the region of the Asian monsoon anticyclone, the correlation coefficients of MLS(O_3)/CLaMS(O_3) are somewhat higher than those of MLS(CO)/ CLaMS(CO). Reasons for this observation could be deficiencies in MLS CO data (v3) in the lower stratosphere as found by Schwartz et al. (2015), who detect a lack of expected signatures in MLS (v3) CO in the context of double tropopauses e. g. on the poleward edge of the Asian monsoon anticyclone and suggest that these deficiencies could be related to unexpectedly weak equator-to-pole gradients of MLS CO in the lower stratosphere (Hegglin and Tegtmeier, 2015). Differences between MLS(CO)/CLaMS(CO) and MLS(O_3)/CLaMS(O_3) correlations could also be caused by limitations in the convective transport of CO in ERA-Interim reanalysis data (see discussion in Sect. 4) or by lower boundary conditions for CO (see Sect. 2.1). '

Page 13, l6-25: The discussion in this paragraph is a little odd because you *indeed find anti-correlation, i.e. the data are the more closely "correlated" the lower the correlation coefficient is. This, however, is not expressed correctly (e.g. l10/11: "During the formation of the anticyclone the correlation coefficients increase ... "; in fact they decrease because they change from -0.2 to -0.8). I suggest to mention the anti-correlation once at the beginning of the para, and then refer to the absolute values of the correlation coefficient abs(r) for the rest of the para.*

We revised this paragraph as follows:

'Fig. 5 shows that the spatial distribution of PV and CLaMS CO is strongly anticorrelated during the formation (-0.89 to -0.95), the existence (-0.74 to -0.93) and the breakup (-0.68 to -0.89) of the Asian monsoon anticyclone. In the course of the Asian monsoon season, a strong anticorrelation between the spatial distribution of low PV and and high percentages of the emission tracer for India/China of -0.71 to -0.87 is found. During the formation of the anticyclone the correlation coefficients decrease because the emission tracer has to be transported up to the UTLS. The increase of the correlation coefficients after the breakup is caused by the lack of convection in Asia occurring during the monsoon season (see comparison between MLS and CLaMS in Sect. 3.1). In contrast, the correlation coefficient between the spatial distribution of PV and the emission tracer for Southeast Asia shows a completely different behaviour. During the formation of the Asian monsoon the contributions of the emission tracer for Southeast Asia decrease similarly as for the emission tracer for India/China. During the existence of the anticyclone a strong anticorrelation with a correlation coefficient up to -0.90 is calculated at the early- and late-phase of the anticyclone, however in early August (mid-phase) the spatial distributions of PV and the emission tracer for Southeast Asia are uncorrelated (indicated by the black dashed line in Fig. 5). This shows that in the mid-phase of the Asian monsoon anticyclone the spatial distribution of air masses originating in Southeast Asia is not connected to the region of the Asian monsoon anticyclone indicating that air masses from Southeast Asia experienced upward transport outside of the Asian monsoon anticyclone (see Sect. 2).'

Page 18, l23: Typo: The new sentence should start with a capital A.

done

Page 24, l10: something is odd with this sentence; remove "proceed"?

done

Figure 6, caption: Typo "Twelve"

done

Figure 8, caption: Something is odd with the first sentence of the caption, are there parts of the sentence missing?

done

References

Bergman, J. W., Fierli, F., Jensen, E. J., Honomichl, S., and Pan, L. L.: Boundary layer sources for the Asian anticyclone: Regional contributions to a vertical conduit, J. Geophys. Res., 118, 2560–2575, doi:10.1002/jgrd.50142, 2013.

Bergman, J. W., Pfister, L., and Yang, Q.: Identifying robust transport features of the upper tropical troposphere, J. Geophys. Res., 120, 6758–6776, doi:10.1002/2015JD023523, 2015.

Chen, B., Xu, X. D., Yang, S., and Zhao, T. L.: Climatological perspectives of air transport from atmospheric boundary layer to tropopause layer over Asian monsoon regions during boreal summer inferred from Lagrangian approach, Atmos. Chem. Phys., pp. 5827–5839, doi:10.5194/acp-12-5827, 2012.

Dee, D. P., Uppala, S. M., Simmons, A. J., Berrisford, P., Poli, P., Kobayashi, S., Andrae, U., Balmaseda, M. A., Balsamo, G., Bauer, P., Bechtold, P., Beljaars, A. C. M., van de Berg, L., Bidlot, J., Bormann, N., Delsol, C., Dragani, R., Fuentes, M., Geer, A. J., Haimberger, L., Healy, S. B., Hersbach, H., Holm, E. V., Isaksen, L., Kallberg, P., Koehler, M., Matricardi, M., McNally, A. P., Monge-Sanz, B. M., Morcrette, J.-J., Park, B.-K., Peubey, C., de Rosnay, P., Tavolato, C., Thepaut, J.-N., and Vitart, F.: The ERA-Interim reanalysis: configuration and performance of the data assimilation system, Q. J. R. Meteorol. Soc., 137, 553–597, doi: 10.1002/qj.828, 2011.

Fadnavis, S., Schultz, M. G., Semeniuk, K., Mahajan, A. S., Pozzoli, L., Sonbawne, S., Ghude, S. D., Kiefer, M., and Eckert, E.: Trends in peroxyacetyl nitrate (PAN) in the upper troposphere and lower stratosphere over southern Asia during the summer monsoon season: regional impacts, Atmos. Chem. Phys., 14, 12 725–12 743, doi:10.5194/acp-14-12725-2014, 2014.

Li, Q., Jiang, J. H., Wu, D. L., Read, W. G., Livesey, N. J., Waters, J. W., Zhang, Y., Wang, B., Filipiak, M. J., Davis, C. P., Turquety, S., Wu, S., Park, R. J., Yantosca, R. M., and Jacob, D. J.: Convective outflow of South Asian pollution: A global CTM simulation compared with EOS MLS observations, Geophys. Res. Lett., 32, L14 826, doi:10.1029/2005GL022762, 2005.

Orbe, C., Waugh, D. W., and Newman, P. A.: Air-mass origin in the tropical lower stratosphere: The influence of Asian boundary layer air, Geophys. Res. Lett., 42, 4240–4248, doi:10.1002/2015GL063937, 2015.

Park, M., Randel, W. J., Emmons, L. K., and Livesey, N. J.: Transport pathways of carbon monoxide in the Asian summer monsoon diagnosed from Model of Ozone and Related Tracers (MOZART), J. Geophys. Res., 114, D08303, doi:10.1029/2008JD010621, 2009.

Ploeger, F., Konopka, P., Günther, G., Grooß, J.-U., and Müller, R.: Impact of the vertical velocity scheme on modeling transport across the tropical tropopause layer, J. Geophys. Res., 115, D03301, doi:10.1029/2009JD012023, 2010.

Pommrich, R., Müller, R., Grooß, J.-U., Konopka, P., Ploeger, P., Vogel, B., Tao, M., Hoppe, C. M., Günther, G., Spelten, N., Hoffmann, L., Pumphrey, H.-C., Viciani, S., D'Amato, F., Volk, M., Hoor, P., Schlager, H., and Riese, M.: Tropical troposphere to stratosphere transport of carbon monoxide and long-lived trace species in the Chemical Lagrangian Model of the Stratosphere (CLaMS), Geosci. Model Dev., 7, 2895–2916, doi:10.5194/gmd-7-2895-2014, 2014.

Schwartz, M. J., Manney, G. L., Hegglin, M. I., Livesey, N. J., Santee, M. L., and Daffer, W. H.: Climatology and variability of trace gases in extratropical double-tropopause regions from MLS, HIRDLS and ACE-FTS measurements, J. Geophys. Res., 120, 843–867, doi:10.1002/2014JD021964, 2015.

Vogel, B., Günther, G., Müller, R., Grooß, J.-U., Hoor, P., Krämer, M., Müller, S., Zahn, A., and Riese, M.: Fast transport from Southeast Asia boundary layer sources to Northern Europe: Rapid uplift in typhoons and eastward eddy shedding of the Asian monsoon anticyclone, Atmos. Chem. Phys., 14, 12 745–12 762, doi:10.5194/acp-14-12745-2014, 2014.

Manuscript prepared for Atmos. Chem. Phys. Discuss.
with version 2015/04/24 7.83 Copernicus papers of the LaTeX class copernicus.cls.
Date: 1 October 2015

Impact of different Asian source regions on the composition of the Asian monsoon anticyclone and on the extratropical lowermost stratosphere

B. Vogel, G. Günther, R. Müller, J.-U. Grooß, and M. Riese

Forschungszentrum Jülich, Institute of Energy and Climate Research – Stratosphere (IEK-7), Jülich, Germany

Correspondence to: B. Vogel (b.vogel@fz-juelich.de)

Abstract

The impact of different boundary layer source regions in Asia on the chemical composition of the Asian monsoon anticyclone, considering its intraseasonal variability in 2012, is analysed by simulations of the Chemical Lagrangian Model of the Stratosphere (CLaMS) using artificial emission tracers. The horizontal distribution of simulated CO, O_3 and artificial emission tracers for India/China are in good agreement with patterns found in satellite measurements of O_3 and CO by the Aura Microwave Limb Sounder (MLS). Using in addition, correlations of artificial emission tracers with potential vorticity (PV) demonstrates that the emission tracer for India/China is a very good proxy for spatial distribution of trace gases within the Asian monsoon anticyclone. The Asian monsoon anticyclone constitutes a horizontal transport barrier for emission tracers and is highly variable in location and shape. From end-June to early-August, a northward movement of the anticyclone and during September, a strong broadening of the spatial distribution of the emission tracer for India/China towards the tropics is found. In addition to the change of the location of the anticyclone, the contribution of different boundary source regions to the composition of Asian monsoon anticyclone in the upper troposphere strongly depends on its intraseasonal variability and is therefore more complex than hitherto believed. The largest contributions to the composition of the air mass in the anticyclone are found from North India and Southeast Asia at a potential temperature of 380 K. In the early (mid-June to mid-July) and late (September) period of the monsoon season 2012, contributions of emissions from Southeast Asia are highest and in the intervening period (early-August) emissions from North India have the largest impact. Our findings show that the temporal variation of the contribution of different convective regions is ~~memorised~~ imprinted in the chemical composition of the Asian monsoon anticyclone.

Air masses originating in Southeast Asia are found both within and outside of the Asian monsoon anticyclone because these air masses experience in addition to transport within the anticyclone upward transport at the southeastern flank of the anticyclone and in the tropics~~and can be entrained by the outer circulation of the anticyclone~~. Subsequently isen-

tropic poleward transport of these air masses occurs at around 380 K with the result that the extratropical lowermost stratosphere in the Northern Hemisphere is flooded by end of September with air masses originating in Southeast Asia. Even after the breakup of the anticyclonic circulation ($\approx$ end-September), significant contributions of air masses originating in India/China are still found in the upper troposphere over Asia. Our results demonstrate that emissions from India, China and Southeast Asia have a significant impact on the chemical composition of the lowermost stratosphere of the Northern Hemisphere in particular at the end of the monsoon season in September/October 2012.

1 Introduction

The Asian summer monsoon circulation is an important global circulation system in northern summer associated with strong upward transport of tropospheric source gases into the upper troposphere and lower stratosphere (UTLS) region (e.g. Li et al., 2005; Randel and Park, 2006; Park et al., 2007, 2008, 2009). Satellite measurements show that tropospheric trace gases such as water vapour (H_2O), carbon monoxide (CO), nitrogen oxides (NO_x), Peroxyacetyl nitrate (PAN), hydrogen cyanide (HCN), and aerosol are confined by the strong anticyclonic circulation in the UTLS and therefore are isolated from the surrounding air (Rosenlof et al., 1997; Jackson et al., 1998; Park et al., 2004, 2008; Li et al., 2005; Xiong et al., 2009; Randel et al., 2010; Vernier et al., 2011; Bourassa et al., 2012; Fadnavis et al., 2013, 2014). In contrast, stratospheric trace gases such as O_3, HNO_3, or HCl show low concentrations in the anticyclone (Randel and Park, 2006; Park et al., 2008; Liu et al., 2009; Konopka et al., 2010). In general, the Asian monsoon circulation is believed to provide an effective pathway for water vapour and pollutants to the lower stratosphere of the Northern Hemisphere (Bian et al., 2012; Ploeger et al., 2013; Vogel et al., 2014; Uma et al., 2014). The mechanisms for possible transport into the lowermost stratosphere are subject of a longstanding debate (Dethof et al., 1999; Park et al., 2009; Randel et al., 2010; Bourassa et al., 2012; Fairlie et al., 2014; Fromm et al., 2014; Vogel et al., 2014).

Increasing stratospheric water vapour has a significant influence on the climate system (e.g. Forster and Shine, 1999; Shindell, 2001; Smith et al., 2001; Forster and Shine, 2002; Vogel et al., 2012), in particular the variability of water vapour in the lower stratosphere is an important driver of surface climate change (e.g. Solomon et al., 2010; Riese et al., 2012). In addition, increasing stratospheric water vapour plays a crucial role in stratospheric chemistry (e.g. Kirk-Davidoff et al., 1999; Dvortsov and Solomon, 2001; Vogel et al., 2011a). Therefore, it is important to understand transport processes from the Asian monsoon region into the global lower stratosphere.

Moreover, the contribution of different boundary source regions in Asia to the chemical composition of the Asian monsoon anticyclone (e.g. Li et al., 2005; Park et al., 2009; Chen et al., 2012; Bergman et al., 2013; Fadnavis et al., 2014) is currently discussed. Chen et al. (2012) found that most impact at tropopause heights is from emissions originating in the tropical Western Pacific region and the South China Sea, while Bergman et al. (2013) found that air masses originating at the Tibetan Plateau and in India are most important at 100 hPa. Simulations with a chemistry transport model by Park et al. (2009) show that the main surface sources of CO in the Asian monsoon anticyclone are from India and Southeast Asia, whereby the weak contribution of air masses originating from the Tibetan plateau in their analysis is due to the lack of significant surface emissions of CO in this region in their model simulations. Further, air masses from northeast India and southwest China uplifted at the eastern side of the anticyclone could also contribute to the chemical composition of the Asian monsoon anticyclone (Li et al., 2005).

In addition to the impact on the contribution of the Asian monsoon anticyclone, deep convection at the eastern/southeastern side of the Asian monsoon anticyclone is discussed as a pathway for transport of tropospheric air directly into the lower stratosphere by direct convective injection (Rosenlof et al., 1997; Park et al., 2007, 2008; Chen et al., 2012). However, the impact of this transport mechanism on the chemical composition of the lower stratosphere has not been isolated from the exchange between the troposphere and the stratosphere associated with the large-scale Brewer–Dobson circulation (Gettelman et al., 2004; Bannister et al., 2004).

The monsoon and the associated seasonal change of wind and rainfall is characterised by prolonged periods of dry and wet conditions in the range of 2–3 weeks. Extended periods with enhanced precipitation (wet spells) characterise active conditions, while dry spells represent periods when a break in monsoon activity occurs (Goswami, 2012, and references therein). The active and break phases are manifestations of the superposition of large scale northward moving 30 to 60 day oscillations and small scale westward propagating 10 to 20 day variations, however details of this variability are far from being well understood (Goswami, 2012, and references therein). This intraseasonal variability of the monsoon is associated with the strength of the Asian monsoon anticyclone in the UTLS (Goswami, 2012). Further, the evolution over the monsoon season of the anticyclone is characterised by large variability in its extent, strength and location (e.g. Randel and Park, 2006). Garny and Randel (2013) found that the temporal variability of the strength of the anticyclone, as diagnosed by low areas of potential vorticity (PV), is driven by the variability in convection with a period of 30–40 days. Also splittings of the Asian monsoon anticyclone into two separate smaller anticyclones frequently occur each year (e.g. Garny and Randel, 2013).

In this paper, we investigate the following main ~~questions~~question. What is the impact of different boundary layer source regions in Asia on the composition of air in the Asian monsoon anticyclone 2012 considering the intraseasonal variability of the anticyclone? Further, we analyse how both boundary layer source regions in Asia and the Asian monsoon anticyclone affect the chemical composition of the lowermost stratosphere.

The summer 2012 is a good example for ~~normal~~ average monsoon conditions. The rainfall in India was ~~normal~~ medium based on the rainfall data set of 306 rain gauges in India provided by the Indian Institute of Tropical Meteorology in Pune, India[1]. A strong relation between rainfall (droughts or floods) during the Indian summer monsoon to El Niño and La Niña events have been established (e. g. Webster et al., 1998; Kumar et al., 2006).

[1] see e.g.,http://www.tropmet.res.in/~kolli/mol/Monsoon/Historical/air.html

In summer 2012 neutral conditions for the El Niño/Southern Oscillation (ENSO) occurred according to the Oceanic Niño Index (ONI)[2].

To answer our question, we performed simulations with the three-dimensional Lagrangian chemistry transport model (CLaMS) (McKenna et al., 2002b, a; Konopka et al., 2012, and references therein). The paper is organised as follows: Sect. 2 describes the CLaMS simulations and the use of inert artificial tracers of air mass origin to mark boundary layer source regions. In Sect. 3, the evolution of the Asian monsoon anticyclone is described and CLaMS results are compared with measurements from the Aura Microwave Limb Sounder (MLS). Further, the impact of different emission tracers to the composition of the anticyclone is calculated for the entire monsoon season 2012. ~~The~~ Our results are discussed in Sect. 4 and the conclusions are given in Sect. ~~4.~~5.

2 The Chemical Lagrangian Model of the Stratosphere (CLaMS)

2.1 Model description

Model simulations were performed using the Chemical Lagrangian Model of the Stratosphere (CLaMS), a three-dimensional chemistry transport model that was originally developed for the stratosphere (e.g. McKenna et al., 2002b, a; Grooß et al., 2005; Grooß and Müller, 2007) and extended to the troposphere (Konopka et al., 2010, 2012; Pommrich et al., 2014, and references therein). It was shown in previous studies, that CLaMS is very well-suited to simulate strong tracer gradients of chemical species in regions where transport barriers exist like the polar vortex (e.g. Günther et al., 2008; Vogel et al., 2008), the extra-tropical tropopause and in the vicinity of the jet streams (e.g. Pan et al., 2006; Konopka et al., 2010; Vogel et al., 2011b; Konopka and Pan, 2012).

CLaMS is based on a Lagrangian formulation of tracer transport and considers an ensemble of air parcels on a time-dependent irregular grid that is transported by use of 3-D-trajectories. The irreversible part of transport, i.e. mixing, is controlled by the local hor-

[2]see e.g., http://ggweather.com/enso/oni.htm

izontal strain and vertical shear rates with mixing parameters deduced from observations (Konopka et al., 2010, and references therein). Here, we present results of global CLaMS simulations that cover an altitude range from the surface up to 900 K potential temperature ($\approx$ 37 km altitude) with a horizontal resolution of 100 km and a maximum vertical resolution of approximately 400 m at the tropopause. The horizontal winds are taken from the ERA-Interim reanalysis (Dee et al., 2011) provided by the European Centre for Medium-Range Weather Forecasts (ECMWF). In this data set, changes are implemented to improve deep and mid-level convection in ERA-Interim data in contrast to previous reanalysis data (Dee et al., 2011).

Mixing parameter, vertical coordinate, and the cross-isentropic velocity of the model follow the model set-up described by Konopka et al. (2012). Convection in CLaMS is represented by vertical velocities in ERA-Interim reanalysis data. CLaMS employs a hybrid coordinate (ζ), which transforms from a strictly isentropic coordinate Θ to a pressure-based coordinate system (more details see Pommrich et al., 2014).

For this study, the CLaMS simulation includes full stratospheric chemistry (Grooß et al., 2014; Sander et al., 2011) and was initialised on 1 May 2012 based on data from AURA-MLS version 3.3 (Livesey et al., 2011) and ACE-FTS version 3.0 and on results of a multi-annual CLaMS simulation started on 1 October 2001 (Konopka et al., 2010). Global O_3, CO, H_2O, HCl, and N_2O fields are derived from MLS data within ± 2.5 days, while the trajectory-determined synoptic locations have been composed to a $2^\circ \times 6^\circ$ (latitude-longitude) grid. Below $\zeta = 350$ K (equal to $\Theta = 350$ K), these species were taken from the CLaMS multi-annual simulation with a linear transition between $\zeta = 350$ and 400 K (equal to $\Theta = 350$–400 K). CO_2 is initialised from this simulation within the whole vertical domain.

The initialisation of CH_4, NO_y, CFC-11, and CFC-12 was derived from N_2O using correlation fits for different latitude bins derived from ACE-FTS version 3.0 data between April and August 2010 following Grooß et al. (2014). The remaining species and the initial partitioning of the chemical families were taken from correlations and the Mainz 2-D model as described by Grooß et al. (2014). At the upper boundary (900 K potential temperature) AURA-MLS and ACE-FTS measurements and tracer-tracer correlations were used similarly as for the initialisation ~~besides CO which was~~ (see above). CO values at the upper boundary were taken from MLS V3.3 data.

At the lower boundary (surface), O_3 is set to a constant tropospheric value of 4.8×10^{-8} volume mixing ratio representing the ozone mixing ratio at 5 km (Brasseur and Solomon, 2005, p. 619). ~~Water vapour is replaced by~~ ECMWF water vapour is used in lower model levels. Lower boundary conditions for CO and CH_4 are derived from AIRS (Atmospheric Infrared Sounder) satellite measurements version 6 following the approach described by Pommrich et al. (2014).

2.1.1 Emission tracers

The aim of our study is to analyse transport pathways of air masses from boundary layer sources to the Asian monsoon anticyclone and ~~further the~~ subsequently transport of these air masses into the extratropical lowermost stratosphere. Three-dimensional CLaMS simulations were performed to include both the advective transport and the irreversible part of transport, namely mixing. The use of artificial tracers in CLaMS that mark particular regions in the atmosphere allows ~~to quantify~~ the origin of air masses, the pathways, and the transport times to be quantified (Günther et al., 2008; Vogel et al., 2011a).

Here, inert artificial tracers of air mass origin, hereafter referred to as "emission tracers", are introduced that mark globally all land masses in the Earth's boundary layer ($\approx$ 2–3 km above surface following orography corresponding to $\zeta < 120$ K) and thus represent regionally different boundary layer sources regions. Figure 1 shows the geographic locations defined for all 13 emission tracers (red boxes). The latitude and longitude range of each box that represents one emission tracer is listed in Table 1. Further, the remaining tropical regions (20° S $-$ 20° N) over the oceans are also marked by artificial tracers (TPO = Tropical Pacific Ocean, TAO = Tropical Atlantic Ocean, TIO = Tropical Indian Ocean) as indicated by blue lines in Fig. 1. Boundary layer regions not considered by the defined emissions tracers listed in Table 1 are summarised in an emission tracer for the background. Because we are in particular interested in the contributions of different boundary layer source regions in Asia to the composition of air within the Asian monsoon anticyclone, the regions defining emission source regions in Asia are better resolved than in regions elsewhere. The separation in different regions in Asia is chosen to separate regions that are currently discussed in the literature as possible source regions (see Sect. 1). The most important regions for our study are North India (NIN), South India (SIN), East China (ECH), and Southeast Asia (SEA). To discuss the CLaMS results, the percentages of emission tracers for North India (NIN), South India (SIN) and East China (ECH) are sometimes summarised in one emission tracer referred to as "India/China" (India/China = NIN + SIN + ECH).

The artificial emission tracers in CLaMS are designed to identify possible boundary source regions in Asia that could contribute to the composition of the Asian monsoon anticyclone in a particular monsoon season, here as a case study for the year 2012. ~~At each time step of the model (every~~ Every 24 hours (time step for mixing in CLaMS) air masses in the model boundary layer are marked by the different emission tracers, i.~~.~~e. the emission tracer for North India (NIN) of an air parcel in the boundary layer over Northern India is set equal to one (NIN = 1). If an air parcel has left the model boundary layer over North India, the value of the emission tracer for NIN (=1) is transported as like a chemical tracer to other regions of the free troposphere or stratosphere. Successive mixing processes between air masses from North India with air masses originating in other regions of the atmosphere (here NIN= 0) during the course of the simulation yield values of NIN differing from the initial distribution (NIN = 1 or NIN = 0). Therefore, the value of the individual emission tracer counts the percentage of an air masses that originated in the specific boundary layer region since 1 May 2012 considering advection and mixing processes.

3 Results

3.1 Evolution of Asian monsoon anticyclone 2012

The spatio-temporal evolution of the Asian monsoon anticyclone in summer 2012 is inferred from three-dimensional CLaMS simulations using the abovementioned emission tracers for Asia. The CLaMS simulation starts on 1 May 2012 before the formation of the Asian monsoon anticyclone begins during June and ends late October after the breakup of the anticyclone. Deep convection (represented in CLaMS by vertical velocities in ERA-Interim reanalysis data; see Sect. 2.1) leads to strong upward transport of emission tracers from source regions in Asia within the Asian monsoon anticyclone. Our simulation confirms that the extent, strength, and location of the anticyclone is highly variable (e.g. Annamalai and Slingo, 2001; Randel and Park, 2006; Garny and Randel, 2013). In particular, the location and the shape of the anticyclone change from day to day which is demonstrated in the following.

Because the Asian monsoon anticyclone is characterised by low PV, the horizontal distributions of the emission tracer for India/China in comparison to the horizontal distribution of PV is analysed at 380 K potential temperature (≈ 16 km) (see Figs. 2 and 3). The level of 380 K potential temperature is located within the Asian monsoon anticyclone just below the thermal tropopause. To discuss the spatio-temporal evolution of the Asian monsoon anticyclone, 6 days are selected reflecting typical situations of the evolution of the Asian monsoon anticyclone. The 1 July 2012 shows conditions at the beginning of the evolution of the Asian monsoon (early-phase), here the anticyclone is centred over Tibet. The 28 July, 2 August and 8 August 2012 are days in the mid-phase of the monsoon season, ~~here~~ when a strong asymmetric anticyclone, a symmetric anticyclone centred over Iran and an anticyclone split into two smaller anticyclones are found. ~~On 12 September 2012 conditions~~ Conditions during the late-phase of the monsoon ~~and on 7 October 2012 the~~ are shown for the 12 September 2012. The situation after the breakup of the anticyclone occurring end-September are shown ~~.~~ using the example of 7 October 2012.

On 1 July 2012 (Fig. 2, top), the anticyclone is centred over Tibet. The northern flank of the anticyclone border on the subtropical westerly jet and the southern flank to the equatorial easterly jet. In our study, the region of strongest gradients in the horizontal distribution of emission tracers from Asia represent the edge of the anticyclone at 380 K. A value of 4.5 PVU (thick white line) is introduced which is in agreement with the upper limit of the PV values derived by Ploeger et al. (2015) to mark the transport barrier for the Asian monsoon anticyclone 2012 at 380 K (more details see Sect. 3.2.1). Filaments consisting of air masses characterised by low PV values (< 4.5 PVU) and enhanced emissions from India/China occur both at the western and eastern flank of the anticyclone.

On 28 July 2012 (Fig. 2, 2nd row), the horizontal distribution of high percentages of emission tracers for India/China shows an elongated structure with maxima at its two endpoints located over Northeast Africa and Southeast China (red coloured). The shape of the PV isoline of 4.5 PVU includes two anticyclones situated close together.

After 28 July 2012, the western peak is transported eastwards and the eastern peak moves westwards and both peaks merge in one location in early August. On 2 August 2012 (see Fig. 2, 3rd row), the anticyclone again has a more symmetric shape and is centred over Iran and Afghanistan. The spatial distribution of emission tracers for India/China shows two regions with maximum values one in the core of the anticyclone over Iran and Afghanistan and another smaller within the anticyclone farther northeast over China. This pattern is a remnant of the elongated structure found in the distribution of emission tracers for India/China on 28 July 2012 caused by the double peak structure of the Asian monsoon anticyclone. This small-scale structure found in the horizontal distribution of emission tracers for India/China is also evident in the spatial distribution of low PV values. On 8 August 2012 (see Fig. 2, bottom), the Asian monsoon anticyclone is split into two smaller anticyclones, one centred over the northern Middle East (Iraq/Iran) and a second one over East China.

In the late-phase of the Asian monsoon anticyclone, on 12 September 2012 the spatial distribution of the emission tracer for India/China is shifted towards the tropics compared to the mid-phase as shown in Fig. 3 (top).

In 2012, the breakup of the Asian monsoon anticyclone occurred in late September. Figure 3 (bottom) shows the spatial distribution of the emission tracers for India/China at 380 K after the breakup on 7 October 2012. The breakup of the anticyclone or the disappearance of the transport barrier goes along with the spread of the emission tracers for India/China at 380 K within the mid-latitudes of the Northern Hemisphere and in the tropics. High percentages of the emission tracers for India/China are found over the Pacific Ocean and over the east cost of North America along the subtropical westerly jet ~~. The subtropical~~

Discussion Paper | Discussion Paper | Discussion Paper | Discussion Paper |

~~jet is in addition a transport barrier for the transport further polewards into the lowermost stratosphere of air masses originating in the boundary layer in India/China~~and in filaments separated at the northeast flank from the Asian monsoon anticyclone (Vogel et al., 2014) . In addition, air masses originating in the boundary layer in India/China could penetrate into the upwelling in the deep branch of the Brewer–Dobson circulation and ~~could in this way reach the upper~~ thus could be transported further up into the stratosphere.

3.1.1 Comparison to MLS measurements

To compare our simulation with MLS O_3 and CO measurements (Version 3.3) (Livesey et al., 2008), pattern correlation coefficients between MLS measurements and CLaMS results, namely MLS(CO)/CLaMS(CO), MLS(O_3)/CLaMS(O_3) and MLS(CO)/CLaMS(India/China), were calculated between 360 and 400 K potential temperature (see Fig. 4). It is expected from satellite measurements that CO mixing ratios are higher within the Asian monsoon anticyclone than outside and vice versa for O_3 indicating that air masses inside the anticyclone have a stronger tropospheric characteristic than air masses in the UTLS outside of the anticyclone. At all days between 1 May 2012 and 31 October 2012, MLS measurements of O_3 and CO in a region between 15 and 50° N and 0 and 140° E (shown as black rectangle in Fig. 2) between 360 and 400 K potential temperature are correlated to CLaMS results as described in the following. At each day, CLaMS results are interpolated on locations of the MLS measurements transformed to synoptic 12:00 UTC positions. For each day, both MLS measurements and CLaMS results are normalised so that the maximum value of each trace gas is equal one. Afterwards the linear Pearson correlation coefficient r(t) between MLS measurement and CLaMS results is calculated for each day. This procedure allows the spatial distribution of trace gases to be compared neglecting possible differences in the absolute mixing ratios between model and measurement and to compare the spatial distribution of different quantities such as measured CO and simulated emission tracers (here India/China).
Correlation coefficients r(t) ranging between 0.72 and 0.86 were calculated for MLS(O_3)/CLaMS(O_3) during the monsoon season 2012 between end of June and

end of September. Before the monsoon season in early May an even higher correlation coefficient up to 0.95 was found ~~.~~ for MLS(O_3)/CLaMS(O_3) most likely caused by the fact that the initial O_3 fields in CLaMS for 1 May 2012 are derived from MLS data (see 2.1). Correlation coefficients of 0.57 to 0.81 were calculated for both MLS(CO)/CLaMS(CO) and MLS(CO)/CLaMS(India/China) between end of June and end of September. These high correlation coefficients confirm that CLaMS has the capability of simulating the spatial distribution of tropospheric trace gases such as CO and stratospheric trace gases like O_3 measured by MLS. In the region of the Asian monsoon anticyclone, the correlation coefficients of MLS(~~O3~~O_3)/CLaMS(~~O3~~O_3) are somewhat higher than those of MLS(CO)/CLaMS(CO). Reasons for ~~that~~ this observation could be deficiencies in MLS CO data (v3) in the lower stratosphere as ~~suggested by Hegglin and Tegtmeier (2015)~~ found by Schwartz et al. (2015) , who detect a lack of expected signatures in MLS (v3) CO in the context of double tropopauses e. g. on the poleward edge of the Asian monsoon anticyclone and suggest that these deficiencies could be related to unexpectedly weak equator-to-pole gradients of MLS CO in the lower stratosphere (Hegglin and Tegtmeier, 2015) . Differences between MLS(CO)/CLaMS(CO) and MLS(O_3)/CLaMS(O_3) correlations could also be caused by limitations in the convective transport of CO in ERA-Interim reanalysis data (see discussion in Sect. 4) or by lower boundary conditions for CO (see Sect. 2.1). To illustrate the good agreement between CLaMS and MLS, the same horizontal cross-sections as in Figs. 2 and 3 at 380 K potential temperature for MLS CO and O_3 as well as for CLaMS CO and O_3 are shown in the Supplement of this paper.

~~A remarkable good correlation between the emission tracers for India/China is simulated in regions where high values of are measured indicating that the emission tracer for India/China is a very good proxy for the spatial distribution of tropospheric trace gases measured in the Asian monsoon anticyclone.~~ The correlation coefficient of MLS(CO)/CLaMS(India/China) increases from 0 to ≈ 0.8 during the formation of the Asian monsoon anticyclone, as expected because in the model the tracer has first to be transported from the ground to the UTLS. After the breakup of the monsoon anticyclone the correlation coefficient of MLS(CO)/CLaMS(India/China) decreases because further upward transport of the tracer for India/China does not occur due the ~~the~~ missing convection in this region and therefore the spatial CO distribution in the UTLS is dominated by other processes. During the existence of the Asian monsoon anticyclone, correlation coefficients of MLS(CO)/CLaMS(India/China) between 0.57 and 0.81 are calculated indicating that the spatial distribution of MLS(CO) within the Asian monsoon anticyclone is good represented by the the spatial distribution of the emission tracers for India/China. This model tracer is therefore a good proxy for the spatial distribution of tropospheric trace gases measured in the Asian monsoon anticyclone.

3.1.2 Different phases of the Asian monsoon anticyclone

To link the temporal variation of the spatial distribution of the emission tracers ~~also~~ to areas of low PV during the entire Asian monsoon period 2012, pattern ~~correlation~~ correlations between PV and the emission tracer for Indian/China (red), the emission tracer Southeast Asia (grey) and CLaMS CO (blue) are calculated as shown in Fig. 5. The correlation coefficients are calculated in a region between 15 and 50° N and 0 and 140° E (shown as black rectangle in Fig. 2) at 380 K similar ~~as for~~ to the MLS/CLaMS correlations described above. For each day, CLaMS results and PV are interpolated on 1 $\times$ 1 latitude longitude grid at 380 K and thereafter normalised to one.

Fig. 5 shows that the spatial distribution of PV and CLaMS CO is ~~very well correlated~~ strongly anticorrelated during the formation (~~-0.89 to -0.95~~ -0.89 to -0.95), the existence (~~-0.74 to -0.93~~ -0.74 to -0.93) and the breakup (~~-0.68 to -0.89~~ -0.68 to -0.89) of the Asian monsoon anticyclone. In the course of the Asian monsoon season, a ~~good correlation~~ strong anticorrelation between the spatial distribution of low PV and and high percentages of the emission tracer for India/China of ~~-0.71 to -0.87~~ -0.71 to -0.87 is found. During the formation of the anticyclone the correlation coefficients ~~increases~~ decrease because the emission tracer has to be transported up to the UTLS. The ~~decrease~~ increase of the correlation coefficients after the breakup is caused by the ~~missing~~ lack of convection in Asia occurring during the monsoon season (see comparison between MLS and CLaMS in Sect. 3.1). In contrast, the correlation coefficient between the spatial distribution of PV and the emission tracer for Southeast Asia shows a completely different behaviour. During the formation of the Asian monsoon the contributions of the emission tracer for Southeast Asia ~~increase~~ decrease similarly as for the emission tracer for India/China. During the existence of the anticyclone a ~~high~~ strong anticorrelation with a correlation coefficient up to ~~-0.90~~ -0.90 is calculated at the early- and late-phase of the anticyclone, however in early August (mid-phase) the ~~correlation between the spatial distribution~~ spatial distributions of PV and the emission tracer for Southeast Asia ~~almost vanishes~~ are uncorrelated (indicated by the black dashed line in Fig. 5). This shows that in the mid-phase of the Asian monsoon anticyclone the spatial distribution of air masses originating in Southeast Asia is not connected to the region of the Asian monsoon anticyclone indicating that air masses from Southeast Asia experienced upward transport outside of the Asian monsoon anticyclone (see Sect. 3.2).

~~The good correlation~~ In the course of the Asian monsoon season, the strong correlation and anticorrelation found between the emission tracer for India/China and MLS ~~measurements~~ CO measurements with correlation coefficients between 0.57 and 0.81 as well as PV ~~confirms~~ with correlations coefficients between -0.71 to -0.87 indicate that the spatial distribution of the emission tracer for India/China is a ~~very~~ good proxy for the location and shape of Asian monsoon anticyclone from end-June to end-September.

Figure 6 shows twelve-day mean values of the emission tracer for India/China and PV during different phases of the Asian monsoon anticyclone. A slight geographical northwards shift of the spatial distribution of the emission tracer for India/China from the early-phase of the anticyclone from end-June/early-July to early-August (mid-phase) is found. Further in early-September, the late-phase of the anticyclone, a much broader spatial distribution of the emission tracer for India/China is found, in particular the southern edge of the anticyclone is shifted towards the tropics. In early-October after the breakup of the anticyclone, still high percentages of the emission tracer for India/China are found over India, China and the Pacific Ocean.

Animations showing the temporal evolution (on a daily basis) of the contribution of emission tracers for India/China, Southeast Asia and PV at 380 K potential temperature on the

Northern Hemisphere during the Asian monsoon season 2012 (1 May 2012–late October 2012) are available as a Supplement of this paper showing the intraseasonal variability of the Asian monsoon anticyclone. In the next sections, the spatial distribution of different emission tracers for Asia within the Asian monsoon anticyclone and the temporal evolution of all tracers within the Asian monsoon anticyclone from May until late October 2012 are discussed.

3.2 Impact of different emission tracers to the composition of the Asian monsoon anticyclone

To analyse the possible impact of different boundary layer source regions in Asia, in particular the specific importance of Southeast Asia, to the composition of the Asian monsoon anticyclone, the horizontal distributions of emission tracers are discussed at 380 K potential temperature using four days introduced in the previous section (1 July, 2 and 8 August, and 12 September 2012, see Sect. 3.1). The emission tracers for North India, South India, and East China show in ~~principle~~ general the same horizontal patterns, therefore here we show only emissions from North India. However, their individual contributions to the composition of the anticyclone differ from tracer to tracer and are time dependent (see Sect. 3.2.1). In the previous section (Sect. 3.1), it is shown that the spatial distribution of the emission tracer for Southeast Asia has a fundamentally different behaviour than the distribution for emission tracers for North India, South India, and East China at 380 K potential temperature (see Fig. 5).

Figure 7 shows the horizontal distribution of emission tracers for North India (NIN) (left) and Southeast Asia (SEA) (right) at 380 K potential temperature over Asia for the four chosen days. In the early-phase on 1 July 2012 (Fig. 7, top), air masses from boundary layer sources in North India and Southeast Asia are confined within the Asian monsoon anticyclone and within the filaments at its western and eastern flank. Air masses influenced by boundary layer sources from Southeast Asia are ~~in addition~~ also found in the tropics. Within the anticyclone the emission tracer for Southeast Asia has the largest contribution at 380 K, followed by the emission tracers for North India. ~~The contributions of the emissions tracer~~

~~for South India is in the same order of magnitude as for North India and the lowest fraction is found for the emission tracer for East China (not shown here).~~

Similar ~~as for~~ to the distribution on 1 July 2012, the distribution of the emission tracer for North India on 2 August 2012 in the mid-phase at 380 K (Fig. 7, 2nd row, left) ~~the distribution of the emission tracer for North India~~ is also confined within the Asian monsoon anticyclone. ~~Filaments containing enhanced contributions of the emission tracer for North India exist also at the western and eastern flank of the anticyclone. Contrary to the~~ In contrast to 1 July~~at the beginning of August~~, the highest percentages of emission tracers within the anticyclone at the beginning of August are from North India and East China (not shown here), thus the impact of boundary sources located more northwards is larger than the impact of boundary sources from Southeast Asia and South India (not shown here).

Further on 2 August 2012 at 380 K, the spatial distribution of the emission tracers for North India shows two regions with maximum values, one in the core of the anticyclone over Iran and Afghanistan and another within the anticyclone farther northeast over China which is a remnant of a double peak structure found on 28 July 2012 as discussed above in Sect. 3.1.

On 2 August 2012, the horizontal distribution of the emission tracer for Southeast Asia is completely different compared to the 1 July 2012. On 2 August 2012 (Fig. 7, 2nd row, right), the contributions of the emission tracer for Southeast Asia has a local minimum in the core of the anticyclone surrounded by enhanced percentages of the emission tracer for Southeast Asia at the edge of the anticyclone in particular at the southeast edge of the anticyclone and in the western and eastern filaments of the anticyclone. This is in contrast to the emission tracer for North India (and East China, not shown here) ~~having~~ which have large contributions in the core and low values at the edge. Therefore, the spatial distribution of the emission tracer for Southeast Asia within the anticyclone is like a negative image to the spatial distribution of the emission tracer for North India. Further looking at a wider geographical scale, large contributions of the emission tracer for Southeast Asia are found south of the anticyclone in the tropics, over the Pacific Ocean and west of the anticyclone over the South Atlantic Ocean.

On 8 August 2012 (Fig. 7, 3rd row), the Asian monsoon anticyclone is split into two smaller anticyclones. Apart from the double peak structure, the spatial distribution of the emission tracer for North India and Southeast Asia is similar to the distribution on 2 August 2012, i. e. high contributions from North India and low contributions from Southeast Asia are found within both cores of the anticyclones. Also here, remarkable are high percentages of the emission tracer for Southeast Asia appear at the edge of the two anticyclones. Thus at the beginning of August 2012, the percentage of emission tracers for North India and East China (not shown here) outweigh the percentage of the emission tracers from further south for Southeast Asia and South India (not shown) inside the anticyclone in contrast to the conditions in the early-phase on 1 July.

Air masses originating in Southeast Asia can experience strong uplift by deep convection (e.g. Park et al., 2007; Li et al., 2005) or typhoons (Vogel et al., 2014). If an air parcel is uplifted at the edge of the Asian monsoon to altitudes high enough, it can be entrained into the anticyclonic circulation and subsequent clockwise transport of the air ~~parcel~~ parcels around the outer edge of the anticyclone occurs. The edge of the anticyclone acts here as a strong transport barrier as evident in the strong gradients of the different emission tracers at the edge of the anticyclone. The transport barrier acts in both directions, namely for inward transport apparent in the tracer distribution from Southeast Asia and for outward transport apparent in the tracer distribution for North India (see Fig. 7, 2nd and 3rd row). Further, air masses originating in the boundary layer in Southeast Asia are uplifted in the tropics at locations where they do not reach the Asian monsoon anticyclone. A ~~subsequently~~ subsequent isentropic poleward transport of these air masses from the tropics to the region of the Asian monsoon anticyclone is evident in the CLaMS simulation.

On 12 September 2012 (see Fig. 7, bottom) during the late-phase, the anticyclone is broadened to the south compared to the area of the Asian monsoon anticyclone in July and August. In the core of the Asian monsoon anticyclone, the main contributions are emission tracers for Southeast Asia and North India followed by East China (not shown). A smaller percentage is found for the emission tracer for South India (not shown).

Further, on 12 September 2012 at the end of the monsoon season, the spatial distribution of the emission tracer for Southeast Asia at 380 K is very different compared to the distributions of the emission tracer for North India in particular within the Northern Hemisphere. During the late-phase of the anticyclone, contributions of the emission tracers for North India are still trapped within the anticyclone. As discussed before, air masses originating in the boundary layer in Southeast Asia are uplifted both within the Asian monsoon anticyclone and elsewhere in the tropics. Uplift in the tropics and subsequent isentropic poleward transport at around 380 K yield propagation of air masses originating in the boundary layer of Southeast Asia to mid-latitudes. Fig. 7 (bottom) shows that on 12 September 2012 in the entire northern hemisphere contributions from Southeast Asia between 6-10 % are found. Therefore, the extratropical lowermost stratosphere in the Northern Hemisphere is flooded by end of September with air masses from Southeast Asia. ~~as~~ As a result, high percentages of the emission tracer for Southeast Asia are more widely distributed compared to the distribution of the emission tracers for North India, South India and East China.

3.2.1 Temporal evolution of different emission tracers

~~After presenting~~ The artificial emission tracers in CLaMS are designed to identify possible boundary source regions in Asia that could contribute to the composition of the Asian monsoon anticyclone during the monsoon season 2012 (as defined in Sect. 2.1.1) considering advection and mixing processes. By this technique contributions of the boundary layer with a transport time from the boundary to the UTLS in the range of one monsoon period (contributions from the boundary layer that are released after 1 May 2012) are covered by the artificial tracers used here. Therefore, the composition of different emission tracers within the Asian monsoon anticyclone is a fingerprint of the regional and temporal variations of convective processes causing strong upward transport within the Asian monsoon anticyclone in summer 2012.

After presenting in the last Sect. 3.2 the spatial distribution of the emission tracers for four selected days, we discuss the temporal evolution of ~~different~~ all emission tracers within the Asian monsoon anticyclone in 2012. In the previous sections, it is shown that the area enclosed by the 4.5 PVU isoline constitutes a good upper boundary for the area within the Asian monsoon anticyclone at 380 K showing enhanced contributions of emission tracers for India/China within the Asian monsoon anticyclone. Ploeger et al. (2015) inferred a mean value of 3.8 PVU to mark the transport barrier for the Asian monsoon anticyclone 2012 at 380 K using the PV gradient and horizontal circulation. However, the PV value marking the transport barrier changes from day to day with maximum PV values up to 4.4–4.6 PVU and could only be deduced for a period from 20 June to 20 August 2012 (Ploeger et al., 2015). In our study, a value of 4.5 PVU is used which is in agreement with the upper limit of the PV values derived by Ploeger et al. (2015) and is extrapolated to early June and September/October 2012.

Therefore, to calculate the percentage of different emission tracers within the Asian monsoon anticyclone at 380 K, we use the following assumption. Mean values of all emission tracers are calculated in Asia for the region between 15 and 50° N and 0 and 140° E (at 380 ± 0.5 K, shown as black rectangle in Fig. 7). In addition to this geographical limit (black rectangle), PV values lower than 4.5 PVU are required for an air parcel to contribute to the mean values of the different emission tracers within the Asian monsoon anticyclone for each day as shown in Fig. 8.

The contribution of different emission tracers from Asia within the anticyclone differ in time and from tracer to tracer (Fig. 8). The temporal evolution shows that significant contributions of the emission tracer for Southeast Asia (black) are found within the Asian monsoon anticyclone at 380 K potential temperature end of May that is roughly 2 weeks before contributions of the emission tracers for North India (red), South India (blue), and East China (green) reach at that level of potential temperature. At the beginning of the Asian monsoon period in June/early July, contributions of air masses originating in South Asia dominate within the anticyclone with maximum percentages of emission tracers on average of 13 % for Southeast Asia (black) and 6.5 % for South India (blue) at 380 K. During July 2012, the contributions of emission tracers for the south decrease to 10 % (Southeast Asia) and 6 % (South India) and contributions of emission tracers for the north, for North India (red) and East China (green) increase up to 18 and 10 %, respectively, until early August. During August 2012, the percentage of the emission tracers for the south rise again until the breakup of the anticyclone which occurred end of September in contrast to decreasing contributions of emission tracers for North India. Our simulations show that a south-north shift in the contribution of different emission tracers for Asia within the Asian monsoon anticyclone occurred during the summer 2012 and also a slight northward shift of the anticyclone itself. This behaviour is possibly linked to the northward moving long-term interseasonal variations (30 to 60 day oscillations) found in climatological analyses of monsoon activity like convection and rainfall (e.g. Goswami, 2012, and references therein).

During August and September 2012, contributions of the emission tracer for North India (red) decrease in ~~principle~~general, however short-term intraseasonal variations (10–20 days) as a local phenomenon are found. We suggest that these oscillations are most likely connected to the short-term westward propagating intraseasonal variations (10–20 days) of the Asian summer monsoon found on a smaller horizontal scale (e.g. Goswami, 2012, and references therein). In the same time period, contributions of the emission tracer for East China show a slight increase with maximum percentages end of September.

At the end of September 2012, the contributions of emission tracers for North India, South India, and East China start to decrease caused by the breakup of the Asian monsoon anticyclone and the missing upward transport within the anticyclone. In contrast to these tracers, the contribution of emission tracers for Southeast Asia increases continuously up to 23 % from its minimum percentage of 10 % in late August until end of October. In early October, the anticyclone had already dissolved, however the contributions of the emission tracer for Southeast Asia still rise. The reason for this increase is that air masses originating in the boundary layer in Southeast Asia experienced in addition to the upward transport in the Asian monsoon anticyclone itself, uplift in the tropics and rapid uplift over the Pacific Ocean. The contribution of the emission tracer for the Tropic Pacific Ocean (TPO) increases after the breakup of the anticyclone (yellow) indicating a strong uplift of air masses in the tropical Pacific. The influence of other land masses + tropical Atlantic and Indian Ocean (dark grey line in Fig. 8) and of the background (light grey) is of minor importance throughout the considered time period.

The conclusions deduced from the temporal evolution of emission tracers do not depend on the precise value of 4.5 PVU. Very similar results were obtained for a choice of 3.8 PVU. Further, even if no PV criterion is applied and all air parcels within the geographical limits (black rectangle in Fig. 2, 3, and 7) are considered to calculate the mean values, the same qualitative evolution of the contributions of different emission tracers emerges within the anticyclone at 380 K. However ~~then~~ when using only the geographical limits, highest contributions from Southeast Asia up to 11% and 19% are calculated in mid-June/mid-July and October, respectively. The contribution of air masses from North India has also its maximum in the intervening period from mid-July to mid-August and reaches values up to 13% (not shown here).

~~The artificial emission tracers in CLaMS are designed to identify possible boundary source regions in Asia that could contribute to the composition of the Asian monsoon anticyclone during the monsoon season 2012 (as defined in Sect. 2.1.1) considering advection and mixing processes. For example, the contribution of the emission tracer for Southeast Asia dominates in June, demonstrating that in June upward transport or convection is comparably strong in Southeast Asia compared to other regions in Asia. By this technique contributions of the boundary layer with a transport time from the boundary to the UTLS longer than one monsoon period (contributions from the boundary layer that are released before 1 May 2012) are not covered by the artificial tracers used here. Therefore, the composition of different emission tracers within the Asian monsoon anticyclone is a fingerprint of the regional and temporal variations of convective processes causing strong upward transport within the Asian monsoon anticyclone in summer 2012.~~

The sum of all emission tracers shown in Fig. 8 is less than 100 % because air masses originating in the free troposphere or stratosphere also contribute to the composition of Asian monsoon anticyclone. For the end of June, a contribution of 35 % of the model boundary layer to the composition of the Asian monsoon anticyclone is calculated as shown in Fig. 9. The remaining 65 % of the composition of the anticyclone is from the free troposphere and the stratosphere. The contribution of the model boundary layer rises up to 55 % in early August and up to 75 % at the end of the monsoon season in late September. Thus at the end of the monsoon season 2012, the chemical composition of the Asian monsoon anticyclone is dominated by contributions of the model boundary layer uplifted during the course of the monsoon season 2012 since 1 May 2012.

4 Discussion

In this paper, we want to show how the impact of different emission tracers changes during the course of the Asian monsoon season 2012 with the focus on the influence of fresh emissions from different regions. Therefore, we selected 1 May 2012 as the start point for our simulation which is before the formation of the Asian monsoon anticyclone. Of course, air masses emitted in the Earth's boundary layer before 1 May 2012 will contribute to the composition of the Asian monsoon anticyclone, however here we aim at quantifying the impact of young air masses in one particular Asian monsoon season that experienced upward transport in the vicinity of the Asian monsoon anticyclone. Our results therefore demonstrate the influence of young air masses on the composition of the Asian monsoon and on the extratropical lowermost stratosphere. Using this approach we could show that on the end of the monsoon season in September up to 75 % of the air masses within the Asian monsoon anticyclone are younger than 5 months (see Fig. 9). That implies that the impact of air masses older than 5 months has only a moderate impacts on the composition of the Asian monsoon anticyclone at the end of the monsoon season. Our results demonstrate that the Asian monsoon system is an effective pathway for transport of air masses from the Earth's surface into the upper troposphere within a few months during the course of the Asian monsoon season 2012.

In contrast to our study, Orbe et al. (2015) used tracers of air mass origin in model simulations to infer the impact of boundary regions in Asia to the tropical lower stratosphere with an approach that the different tracers have equilibrated so that the sum of all tracers of air mass origin is equal to unity within the entire atmosphere (using a spin-up of 20 years). This approach provides for each air parcel the information about the origin within the boundary layer. However, this approach provides no information on the transport times from the boundary layer in Asia to the tropical lower stratosphere. To infer the transport times in the approach by Orbe et al. (2015) , they introduce a boundary impulse response that marks air that left the boundary layer on a certain day (1 July). They infer transport times of one month from the boundary layer in Asia into the tropical lower stratosphere in July when the Asian monsoon is active. In this respect, their pulse serves a similar purpose as our seasonal tracer setup. However, our approach considers all air masses that left the boundary layer over the course of the monsoon season 2012 since May and thus reflects so the meteorological conditions of the entire monsoon season 2012.

In our approach, the absolute percentages of the emission tracers found within the Asian monsoon anticyclone depend on the start point of the model simulations on 1 May 2012. However, the temporal behaviour of the individual emission tracers depends on convective processes causing strong upward transport within the Asian monsoon anticyclone in summer 2012 and are therefore a fingerprint of the regional and temporal variations during the course of the monsoon season. This approach gives insights in the temporal variability of the composition of the Asian monsoon anticyclone over the course of the monsoon period 2012 in addition to earlier studies which analysed the origin of air masses within the Asian monsoon anticyclone for a certain shorter period of the monsoon season (e. g. Li et al., 2005; Bergman et al., 2013) or infer mean values of air mass origin for the entire monsoon season (e. g. Park et al., 2009; Chen et al., 2012; Fadnavis et al., 2014) .

The upward transport and convection in CLaMS is driven by ERA-Interim reanalysis data in which changes are implemented to improve deep and mid-level convection compared to previous reanalysis data (Dee et al., 2011) . However, small-scale rapid uplift in convective cores is not included. We expect that in data sets additionally including the small-scale rapid uplift in convective cores, the uplift of air masses within the Asian monsoon should be even more pronounced. However, previous studies (e. g. Ploeger et al., 2010; Pommrich et al., 2014; Vogel et al., 2014) show that ERA-Interim reanalysis data are well suited to study transport processes in the vicinity of the Asian monsoon anticyclone and in the tropical tropopause layer (TTL). In addition, in CLaMS the diabatic approach with potential temperature as the vertical coordinate

(Pommrich et al., 2014) is used which is suggested to yield more reliable results compared to kinematic calculations (e. g. Ploeger et al., 2010; Bergman et al., 2015) .

5 Conclusions

In this paper, the impact of different boundary layer source regions in Asia to the composition of the Asian monsoon anticyclone 2012 is characterised by CLaMS model simulations using artificial emissions tracers. Our simulations show that the Asian monsoon anticyclone is highly variable in location and shape and the edge of the anticyclone constitutes a ~~remarkable~~ strong transport barrier for artificial emission tracers.

The calculated correlation coefficients indicate good agreement between the horizontal distributions of simulated CO, O_3 and artificial emission tracers for India/China with patterns found in satellite measurements of O_3 and CO by the Aura Microwave Limb Sounder (MLS). For the monsoon season, correlation coefficients r(t) of 0.72-0.86 and 0.57-0.81 were calculated for MLS(O_3)/CLaMS(O_3) and both MLS(CO)/CLaMS(CO) and MLS(CO)/CLaMS(India/China) correlations, respectively. ~~The good correlation found~~In addition in the course of the Asian monsoon season, a strong anticorrelation between the emission tracer for India/China and PV with correlations coefficients between -0.71 to -0.87 are found. These correlation coefficients between the emission tracer for India/China and MLS measurements as well as PV ~~confirms~~ indicate that the spatial distribution of the emission tracer for India/China is a good proxy for the location and shape of Asian monsoon anticyclone. A slight geographical northward shift of the spatial distribution of the emission tracer for India/China from the early-phase of the anticyclone on end-June/early-July to early-August (mid-phase) is found. Further in early-September, during the late-phase of the anticyclone, a much broader spatial distribution is found, in particular the southern edge of the anticyclone is shifted to the tropics. ~~After the breakup of the anticyclone in early-October, still high~~ High percentages for the emission tracer for India/China ~~are~~ located over India, China and the Pacific Ocean are still found after the breakup of the anticyclone in early-October.

In this paper, we could answer the question of what is the impact of different boundary layer sources in Asia to the Asian monsoon anticyclone in summer 2012. The model results show that emissions from North India, South India, East China, and Southeast Asia have ~~an~~ a larger impact on the composition of the Asian monsoon anticyclone ~~in contrast to~~ than emission tracers of all other land masses. The contributions of these different emission tracers on the composition of the anticyclone are highly variable in time, but in general the highest contribution are from North India and Southeast Asia. In the early (≈ June to mid-July) and late period (September/October) of the monsoon season 2012, contributions from Southeast Asia are highest (up to 13% and 23%, respectively, using a value of 4.5 PVU to mark the edge of the anticyclone). In the intervening period (≈ mid-July to mid-August), air masses from North India have the strongest contribution to the composition of the anticyclone (up to 18%). This behaviour is likely caused by the large scale northward moving 30 to 60 day oscillations of the Asian monsoon evident in repeatedly northward-propagating wet spells during the summer monsoon season. Short-term intraseasonal variations (10–20 days) are found in the contribution for air masses originating in North India, which is likely associated to westward propagating 10 to 20 day oscillations of the South Asian summer monsoon found on a smaller horizontal scale. Our simulation confirms that both North India including the Tibetan Plateau (Bergman et al., 2013) and Southeast Asia including the eastern part of Bay of Bengal, South Asian subcontinent, Western Pacific, and the Philippine Seas (Park et al., 2009; Chen et al., 2012) are important source regions for the chemical composition of the Asian monsoon anticyclone. Our simulations demonstrate that the contributions of different boundary source regions to the composition of the Asian monsoon anticyclone show strong intraseasonal variations. Thus the chemical contribution of the Asian monsoon anticyclone is a fingerprint of the regional temporal variation of convective processes. ~~Therefore the processes are~~ The variability of the composition of the Asian monsoon anticyclone over the course of the monsoon season is therefore more complex than hitherto believed.

In addition, emissions from Southeast Asia are found both within the Asian monsoon anticyclone and at the outer edge of the anticyclone. CLaMS simulations show that emissions from Southeast Asia can be rapidly uplifted by deep convection (Li et al., 2005; Chen et al., 2012) or typhoons (Vogel et al., 2014) up to the outer edge of the anticyclone (at around 380 K). Afterwards, the emissions are entrained by the anticyclonic circulation of the Asian monsoon and circulate clockwise, in an upward spiral, at the edge of the Asian monsoon anticyclone around its core (this is also true if the anticyclone is split into two smaller anticyclones). Moreover, our simulations show that air masses originating in Southeast Asia can be uplifted elsewhere in the deep tropics and subsequently spread out during the simulation globally on the tropical side of the subtropical jet stream at around 380 K, in contrast to emissions from North India, South India, and East China that are trapped in the Asian monsoon anticyclone. During the summer 2012, this mechanism caused flooding of the lowermost stratosphere with relatively young air masses originating in Southeast Asia. Finally, after the breakup of the Asian monsoon anticyclone ~~proceed~~ in late September 2012, also emissions from North India, South India, and East China that were trapped before within the Asian monsoon anticyclone were distributed globally within the UTLS.

Our findings demonstrate that emissions from India/China and Southeast Asia carrying moisture and pollution affected by the circulation of the Asian monsoon anticyclone have a significant impact on the chemical compositions of the lowermost stratosphere of the Northern Hemisphere in particular at end of the monsoon season in September/October 2012.

The Supplement related to this article is available online at doi:10.5194/acpd-0-1-2015-supplement.

Acknowledgements. The authors sincerely thank Paul Konopka, Felix Plöger, and Reinhold Spang (all at Research Centre Jülich) for helpful discussions. We thank the MLS scientific team (Aura Microwave Limb Sounder) for providing satellite data and the European Centre of Medium-Range Weather Forcasts (ECMWF) for providing the ERA-Interim reanalysis data. The authors gratefully acknowledge the computing time granted on the supercomputer JUROPA at Jülich Supercomputing Centre (JSC) under the VSR project ID JICG11. Our activities were partly funded by the German

Science Foundation (Deutsche Forschungsgemeinschaft, DFG) under the DFG project LASSO (HALO-SPP 1294/GR 3786).

The article processing charges for this open-access publication were covered by a Research Centre of the Helmholtz Association.

References

Annamalai, H. and Slingo, J. M.: Active/break cycles: diagnosis of the intraseasonal variability of the Asian Summer Monsoon, Clim. Dynam., 18, 85–102, 2001.

Bannister, R. N., O'Neill, A., Gregory, A. R., and Nissen, K. M.: The role of the south-east Asian monsoon and other seasonal features in creating the "tape-recorder" signal in the Unified Model, Q. J. Roy. Meteor. Soc., 130, 1531–1554, 2004.

Bergman, J. W., Fierli, F., Jensen, E. J., Honomichl, S., and Pan, L. L.: Boundary layer sources for the Asian anticyclone: regional contributions to a vertical conduit, J. Geophys. Res., 118, 2560–2575, doi:10.1002/jgrd.50142, 2013.

Bergman, J. W., Pfister, L., and Yang, Q.: Identifying robust transport features of the upper tropical troposphere, J. Geophys. Res., 120, 6758–6776, doi:10.1002/2015JD023523, 2015.

Bian, J., Pan, L. L., Paulik, L., Vömel, H., and Chen, H.: In situ water vapor and ozone measurements in Lhasa and Kunmin during the Asian summer monsoon, Geophys. Res. Lett., 39, L19808, doi:10.1029/2012GL052996, 2012.

Bourassa, A. E., Robock, A., Randel, W. J., Deshler, T., Rieger, L. A., Lloyd, N. D., Llewellyn, E. J. T., and Degenstein, D. A.: Large volcanic aerosol load in the stratosphere linked to Asian monsoon transport, Science, 337, 78–81, doi:10.1126/science.1219371, 2012.

Brasseur, G. and Solomon, S.: Aeronomy of the Middle Atmosphere: Chemistry and Physics of the Stratosphere and Mesosphere, 3rd edn., Springer, Heidelberg, Germany, 2005.

Chen, B., Xu, X. D., Yang, S., and Zhao, T. L.: Climatological perspectives of air transport from atmospheric boundary layer to tropopause layer over Asian monsoon regions during boreal summer inferred from Lagrangian approach, Atmos. Chem. Phys., 12, 5827–5839, doi:10.5194/acp-12-5827-2012, 2012.

Dee, D. P., Uppala, S. M., Simmons, A. J., Berrisford, P., Poli, P., Kobayashi, S., Andrae, U., Balmaseda, M. A., Balsamo, G., Bauer, P., Bechtold, P., Beljaars, A. C. M., van de Berg, L., Bidlot, J., Bormann, N., Delsol, C., Dragani, R., Fuentes, M., Geer, A. J., Haimberger, L., Healy, S. B., Hersbach, H., Holm, E. V., Isaksen, L., Kallberg, P., Koehler, M., Matricardi, M., McNally, A. P., Monge-Sanz, B. M., Morcrette, J.-J., Park, B.-K., Peubey, C., de Rosnay, P., Tavolato, C., Thepaut, J.-N., and Vitart, F.: The ERA-Interim reanalysis: configuration and performance of the data assimilation system, Q. J. Roy. Meteor. Soc., 137, 553–597, doi:10.1002/qj.828, 2011.

Dethof, A., O'Neill, A., Slingo, J. M., and Smit, H. G. J.: A mechanism for moistening the lower stratosphere involving the Asian summer monsoon, Q. J. Roy. Meteor. Soc., 556, 1079–1106, 1999.

Dvortsov, V. L. and Solomon, S.: Response of the stratospheric temperatures and ozone to past and future increases in stratospheric humidity, J. Geophys. Res., 106, 7505–7514, 2001.

Fadnavis, S., Semeniuk, K., Pozzoli, L., Schultz, M. G., Ghude, S. D., Das, S., and Kakatkar, R.: Transport of aerosols into the UTLS and their impact on the Asian monsoon region as seen in a global model simulation, Atmos. Chem. Phys., 13, 8771–8786, doi:10.5194/acp-13-8771-2013, 2013.

Fadnavis, S., Schultz, M. G., Semeniuk, K., Mahajan, A. S., Pozzoli, L., Sonbawne, S., Ghude, S. D., Kiefer, M., and Eckert, E.: Trends in peroxyacetyl nitrate (PAN) in the upper troposphere and lower stratosphere over southern Asia during the summer monsoon season: regional impacts, Atmos. Chem. Phys., 14, 12725–12743, doi:10.5194/acp-14-12725-2014, 2014.

Fairlie, T. D., Vernier, J.-P., Natarajan, M., and Bedka, K. M.: Dispersion of the Nabro volcanic plume and its relation to the Asian summer monsoon, Atmos. Chem. Phys., 14, 7045–7057, doi:10.5194/acp-14-7045-2014, 2014.

Forster, P. and Shine, K. P.: Stratospheric water vapour change as possible contributor to observed stratospheric cooling, Geophys. Res. Lett., 26, 3309–3312, doi:10.1029/1999GL010487, 1999.

Forster, P. and Shine, K. P.: Assessing the climate impact of trends in stratospheric water vapor, Geophys. Res. Lett., 29, 10-1–10-4, doi:10.1029/2001GL013909, 2002.

Fromm, M., Kablick III, G., Nedoluha, G., Carboni, E., Grainger, R., Campbell, J., and Lewis, J.: Correcting the record of volcanic stratospheric aerosol impact: Nabro and Sarychev Peak, J. Geophys. Res., 119, 10343–10364, doi:10.1002/2014JD021507, 2014.

Garny, H. and Randel, W. J.: Dynamic variability of the Asian monsoon anticyclone observed in potential vorticity and correlations with tracer distributions, J. Geophys. Res., 118, 13421–13433, doi:10.1002/2013JD020908, 2013.

Gettelman, A., Kinnison, D., Dunkerton, T. J., and Brasseur, G. P.: Impact of monsoon circulations on the upper troposphere and lower stratosphere, J. Geophys. Res., 109, D22101, doi:10.1029/2004JD004878, 2004.

Goswami, B. N.: South Asian monsoon, in: Intraseasonal Variability in the Atmosphere-Ocean Climate System, 2nd edn., chap. 2, edited by: Lau, W. K. M. and Waliser, D. E., Springer-Verlag, Berlin, Heidelberg, 21–72, 2012.

Grooß, J.-U. and Müller, R.: Simulation of ozone loss in Arctic winter 2004/2005, Geophys. Res. Lett., 34, L05804, doi:10.1029/2006GL028901, 2007.

Grooß, J.-U., Konopka, P., and Müller, R.: Ozone chemistry during the 2002 Antarctic vortex split, J. Atmos. Sci., 62, 860–870, 2005.

Grooß, J.-U., Engel, I., Borrmann, S., Frey, W., Günther, G., Hoyle, C. R., Kivi, R., Luo, B. P., Molleker, S., Peter, T., Pitts, M. C., Schlager, H., Stiller, G., Vömel, H., Walker, K. A., and Müller, R.: Nitric acid trihydrate nucleation and denitrification in the Arctic stratosphere, Atmos. Chem. Phys., 14, 1055–1073, doi:10.5194/acp-14-1055-2014, 2014.

Günther, G., Müller, R., von Hobe, M., Stroh, F., Konopka, P., and Volk, C. M.: Quantification of transport across the boundary of the lower stratospheric vortex during Arctic winter 2002/2003, Atmos. Chem. Phys., 8, 3655–3670, doi:10.5194/acp-8-3655-2008, 2008.

Hegglin, M. I., and Tegtmeier, S. (Eds.): SPARC Data Initiative: Assessment of Stratospheric Trace Gas and Aerosol Climatologies from Satellite Limb Sounders, SPARC Report No. 7, in preparation, 2015.

Jackson, D. R., Driscoll, S. J., Highwood, E. J., Harries, J. E., and Russell III, J. M.: Troposphere to stratosphere transport at low latitudes as studies using HALOE observations of water vapor 1992–1997, Q. J. Roy. Meteor. Soc., 124, 169–192, 1998.

Kirk-Davidoff, D. B., Hintsa, E. J., Anderson, J. G., and Keith, D. W.: The effect of climate change on ozone depletion through changes in stratospheric water vapour, Nature, 402, 399–401, doi:10.1038/46521, 1999.

Konopka, P. and Pan, L. L.: On the mixing-driven formation of the Extratropical Transition Layer (ExTL), J. Geophys. Res., 117, D18301, doi:10.1029/2012JD017876, 2012.

Konopka, P., Grooß, J.-U., Günther, G., Ploeger, F., Pommrich, R., Müller, R., and Livesey, N.: Annual cycle of ozone at and above the tropical tropopause: observations versus simulations with the Chemical Lagrangian Model of the Stratosphere (CLaMS), Atmos. Chem. Phys., 10, 121–132, 2010.

Konopka, P., Ploeger, F., and Müller, R.: Entropy- and static stability-based Lagrangian model grids, in: Geophysical Monograph Series: Lagrangian Modeling of the Atmosphere, edited by Lin, J., vol. 200, pp. 99–109, American Geophysical Union, doi:10.1029/2012GM001253, 2012.

Kumar, K. K., Rajagopalan, B., Hoerling, M., Bates, G., and Cane, M.: Unraveling the Mystery of Indian Monsoon Failure During El Niño, Science, 314, 115–119, doi:10.1126/science.1131152, 2006.

Li, Q., Jiang, J. H., Wu, D. L., Read, W. G., Livesey, N. J., Waters, J. W., Zhang, Y., Wang, B., Filipiak, M. J., Davis, C. P., Turquety, S., Wu, S., Park, R. J., Yantosca, R. M., and Jacob, D. J.: Convective outflow of South Asian pollution: a global CTM simulation compared with EOS MLS observations, Geophys. Res. Lett., 32, L14826, doi:10.1029/2005GL022762, 2005.

Liu, Y., Wang, Y., Liu, X., Cai, Z., and Chance, K.: Tibetan middle tropospheric ozone minimum in June discovered from GOME observations, Geophys. Res. Lett., 36, L05814, doi:10.1029/2008GL037056, 2009.

Livesey, N. J., Filipiak, M. J., Froidevaux, L., Read, W. G., Lambert, A., Santee, M. L., Jiang, J. H., Pumphrey, H. C., Waters, J. W., Cofield, R. E., Cuddy, D. T., Daffer, W. H., Drouin, B. J., Fuller, R. A., Jarnot, R. F., Jiang, Y. B., Knosp, B. W., Li, Q. B., Perun, V. S., Schwartz, M. J., Snyder, W. V., Stek, P. C., Thurstans, R. P., Wagner, P. A., Avery, M., Browell, E. V., Cammas, J.-P., Christensen, L. E., Diskin, G. S., Gao, R.-S., Jost, H.-J., Loewenstein, M., Lopez, J. D., Nedelec, P., Osterman, G. B., Sachse, G. W., and Webster, C. R.: Validation of Aura Microwave Limb Sounder O_3 and CO observations in the upper troposphere and lower stratosphere, J. Geophys. Res., 113, D15S02, doi:10.1029/2007JD008805, 2008.

Livesey, N. J., Read, W. G., Froidevaux, L., Lambert, A., Manney, G. L., Pumphrey, H. C., Santee, M. L., Schwartz, M. J., Wang, S., Cofield, R. E., Cuddy, D. T., Fuller, R. A., Jarnot, R. F., Jiang, J. H., Knosp, B. W., Stek, P. C., Wagner, P. A., , and Wu, D. L.: EOS MLS Version 3.3 Level 2 data quality and description document, Tech. rep., Jet Propulsion Laboratory, available from https://mls.jpl.nasa.gov/data/v3-3_data_quality_document.pdf, 2011.

McKenna, D. S., Grooß, J.-U., Günther, G., Konopka, P., Müller, R., Carver, G., and Sasano, Y.: A new Chemical Lagrangian Model of the Stratosphere (CLaMS): 2. Formulation of chemistry scheme and initialization, J. Geophys. Res., 107, 4256, doi:10.1029/2000JD000113, 2002a.

McKenna, D. S., Konopka, P., Grooß, J.-U., Günther, G., Müller, R., Spang, R., Offermann, D., and Orsolini, Y.: A new Chemical Lagrangian Model of the Stratosphere (CLaMS): 1. Formulation of advection and mixing, J. Geophys. Res., 107, 4309, doi:10.1029/2000JD000114, 2002b.

Orbe, C., Waugh, D. W., and Newman, P. A.: Air-mass origin in the tropical lower stratosphere: The influence of Asian boundary layer air, Geophys. Res. Lett., 42, 4240–4248, doi:10.1002/2015GL063937, 2015.

Pan, L. L., Konopka, P., and Browell, E. V.: Observations and model simulations of mixing near the extratropical tropopause, J. Geophys. Res., 111, D05106, doi:10.1029/2005JD006480, 2006.

Park, M., Randel, W. J., Kinnison, D. E., Garcia, R. R., and Choi, W.: Seasonal variation of methane, water vapor, and nitrogen oxides near the tropopause: Satellite observations and model simulations, J. Geophys. Res., 109, D03302, doi:10.1029/2003JD003706, 2004.

Park, M., Randel, W. J., Gettleman, A., Massie, S. T., and Jiang, J. H.: Transport above the Asian summer monsoon anticyclone inferred from Aura Microwave Limb Sounder tracers, J. Geophys. Res., 112, D16309, doi:10.1029/2006JD008294, 2007.

Park, M., Randel, W. J., Emmons, L. K., Bernath, P. F., Walker, K. A., and Boone, C. D.: Chemical isolation in the Asian monsoon anticyclone observed in Atmospheric Chemistry Experiment (ACE-FTS) data, Atmos. Chem. Phys., 8, 757–764, 2008.

Park, M., Randel, W. J., Emmons, L. K., and Livesey, N. J.: Transport pathways of carbon monoxide in the Asian summer monsoon diagnosed from Model of Ozone and Related Tracers (MOZART), J. Geophys. Res., 114, D08303, doi:10.1029/2008JD010621, 2009.

Ploeger, F., Konopka, P., Günther, G., Grooß, J.-U., and Müller, R.: Impact of the vertical velocity scheme on modeling transport across the tropical tropopause layer, J. Geophys. Res., 115, D03301, doi:10.1029/2009JD012023, 2010.

Ploeger, F., Günther, G., Konopka, P., Fueglistaler, S., Müller, R., Hoppe, C., Kunz, A., Spang, R., Grooß, J.-U., and Riese, M.: Horizontal water vapor transport in the lower stratosphere from subtropics to high latitudes during boreal summer, J. Geophys. Res., 118, 8111–8127, doi:10.1002/jgrd.50636, 2013.

Ploeger, F., Gottschling, C., Grießbach, S., Grooß, J.-U., Günther, G., Konopka, P., Müller, R., Riese, M., Stroh, F., Ungermann, J., Vogel, B., and von Hobe, M.: On deducing the transport barrier in the Asian summer monsoon anticyclone based on isentropic PV-gradients, Atmos. Chem. Phys. Discuss., submitted, 2015.

Pommrich, R., Müller, R., Grooß, J.-U., Konopka, P., Ploeger, F., Vogel, B., Tao, M., Hoppe, C. M., Günther, G., Spelten, N., Hoffmann, L., Pumphrey, H.-C., Viciani, S., D'Amato, F., Volk, C. M., Hoor, P., Schlager, H., and Riese, M.: Tropical troposphere to stratosphere transport of carbon monoxide and long-lived trace species in the Chemical Lagrangian Model of the Stratosphere (CLaMS), Geosci. Model Dev., 7, 2895–2916, doi:10.5194/gmd-7-2895-2014, 2014.

Randel, W. J. and Park, M.: Deep convective influence on the Asian summer monsoon anticyclone and associated tracer variability observed with Atmospheric Infrared Sounder (AIRS), J. Geophys. Res., 111, D12314, doi:10.1029/2005JD006490, 2006.

Randel, W. J., Park, M., Emmons, L., Kinnison, D., Bernath, P., Walker, K. A., Boone, C., and Pumphrey, H.: Asian monsoon transport of pollution to the stratosphere, Science, 328, 611–613, doi:10.1126/science.1182274, 2010.

Riese, M., Ploeger, F., Rap, A., Vogel, B., Konopka, P., Dameris, M., and Forster, P.: Impact of uncertainties in atmospheric mixing on simulated UTLS composition and related radiative effects, J. Geophys. Res., 117, D16305, doi:10.1029/2012JD017751, 2012.

Rosenlof, K. H., Tuck, A. F., Kelly, K. K., Russell III, J. M., and McCormick, M. P.: Hemispheric asymmetries in the water vapor and inferences about transport in the lower stratosphere, J. Geophys. Res., 102, 13213–13234, 1997.

Sander, S. P., Friedl, R. R., Barker, J. R., Golden, D. M., Kurylo, M. J., Wine, P. H., Abbatt, J. P. D., Burkholder, J. B., Kolb, C. E., Moortgat, G. K., Huie, R. E., and Orkin, V. L.: Chemical Kinetics and Photochemical Data for Use in Atmospheric Studies, JPL Publication, 10-6, 2011.

Schwartz, M. J., Manney, G. L., Hegglin, M. I., Livesey, N. J., Santee, M. L., and Daffer, W. H.: Climatology and variability of trace gases in extratropical double-tropopause regions from MLS, HIRDLS and ACE-FTS measurements, J. Geophys. Res., 120, doi:10.1002/2014JD021964, 2015.

Shindell, D. T.: Climate and ozone response to increased stratospheric water vapor, Geophys. Res. Lett., 28, 1551–1554, doi:10.1029/1999GL011197, 2001.

Smith, C. A., Haigh, J. D., and Toumi, R.: Radiative forcing due to trends in stratospheric water vapour, Geophys. Res. Lett., 28, 179–182, 2001.

Solomon, S., Rosenlof, K., Portmann, R., Daniel, J., Davis, S., Sanford, T., and Plattner, G.-K.: Contributions of stratospheric water vapor to decadal changes in the rate of global warming, Science, 327, 1219–1223, doi:10.1126/science.1182488, 2010.

Uma, K. N., Das, S. K., and Das, S. S.: A climatological perspective of water vapor at the UTLS region over different global monsoon regions: observations inferred from the Aura-MLS and reanalysis data, Clim. Dyn., 43, 407–420, doi:10.1007/s00382-014-2085-9, 2014.

Vernier, J.-P., Thomason, L. W., and Kar, J.: CALIPSO detection of an Asian tropopause aerosol layer, Geophys. Res. Lett., 38, L07804, doi:10.1029/2010GL046614, 2011.

Vogel, B., Konopka, P., Grooß, J.-U., Müller, R., Funke, B., López-Puertas, M., Reddmann, T., Stiller, G., von Clarmann, T., and Riese, M.: Model simulations of stratospheric ozone loss caused by enhanced mesospheric NO_x during Arctic Winter 2003/2004, Atmos. Chem. Phys., 8, 5279–5293, doi:10.5194/acp-8-5279-2008, 2008.

Vogel, B., Feck, T., and Grooß, J.-U.: Impact of stratospheric water vapor enhancements caused by CH_4 and H_2 increase on polar ozone loss, J. Geophys. Res., 116, D05301, doi:10.1029/2010JD014234, 2011a.

Vogel, B., Pan, L. L., Konopka, P., Günther, G., Müller, R., Hall, W., Campos, T., Pollack, I., Weinheimer, A., Wei, J., Atlas, E. L., and Bowman, K. P.: Transport pathways and signatures of mixing in the extratropical tropopause region derived from Lagrangian model simulations, J. Geophys. Res., 116, D05306, doi:10.1029/2010JD014876, 2011b.

Vogel, B., Feck, T., Grooß, J.-U., and Riese, M.: Impact of a possible future global hydrogen economy on Arctic stratospheric ozone loss, Energ. Environ. Sci., 5, 6445–6452, doi:10.1039/c2ee03181g, 2012.

Vogel, B., Günther, G., Müller, R., Grooß, J.-U., Hoor, P., Krämer, M., Müller, S., Zahn, A., and Riese, M.: Fast transport from Southeast Asia boundary layer sources to northern Europe: rapid uplift in typhoons and eastward eddy shedding of the Asian monsoon anticyclone, Atmos. Chem. Phys., 14, 12745–12762, doi:10.5194/acp-14-12745-2014, 2014.

Webster, P. J., Magaña, V. O., Palmer, T. N., Shukla, J., Tomas, R. A., Yanai, M., and Yasunari, T.: Monsoon: Processes, predictability, and the prospects for prediction, J. Geophys. Res., 103, 14.451–14.510, 1998.

Xiong, X., Houweling, S., Wei, J., Maddy, E., Sun, F., and Barnet, C.: Methane plume over south Asia during the monsoon season: satellite observation and model simulation, Atmos. Chem. Phys., 9, 783–794, doi:10.5194/acp-9-783-2009, 2009.

Table 1. Latitude and longitude range of artificial boundary layer sources in the CLaMS model, also referred to as "emission tracers". The geographic position of each emission tracer is shown in Fig. 1.

Emission Tracer	Latitude	Longitude
North India (NIN)	20–40° N	55–90° E
South India (SIN)	0–20° N	55–90° E
East China (ECH)	20–40° N	90–125° E
Southeast Asia (SEA)	12° S–20° N	90–155° E
Siberia (SIB)	40–75° N	55–180° E
Europe (EUR)	45–75° N	20° W–55° E
Mediterranean (MED)	35–45° N	20° W–55° E
North Africa (NAF)	0–35° N	20° W–55° E
South Africa (SAF)	36° S–0° N	7–42° E
Madagaskar (MDG)	27–12° S	42–52° E
Australia (AUS)	40–12° S	110–155° E
North America (NAM)	15–75° N	160–50° W
South America (SAM)	55° S–15° N	80–35° W
Tropical Pacific Ocean (TPO)	20° S–20° N	see Fig. 1
Tropical Atlantic Ocean (TAO)	20° S–20° N	see Fig. 1
Tropical Indian Ocean (TIO)	20° S–20° N	see Fig. 1

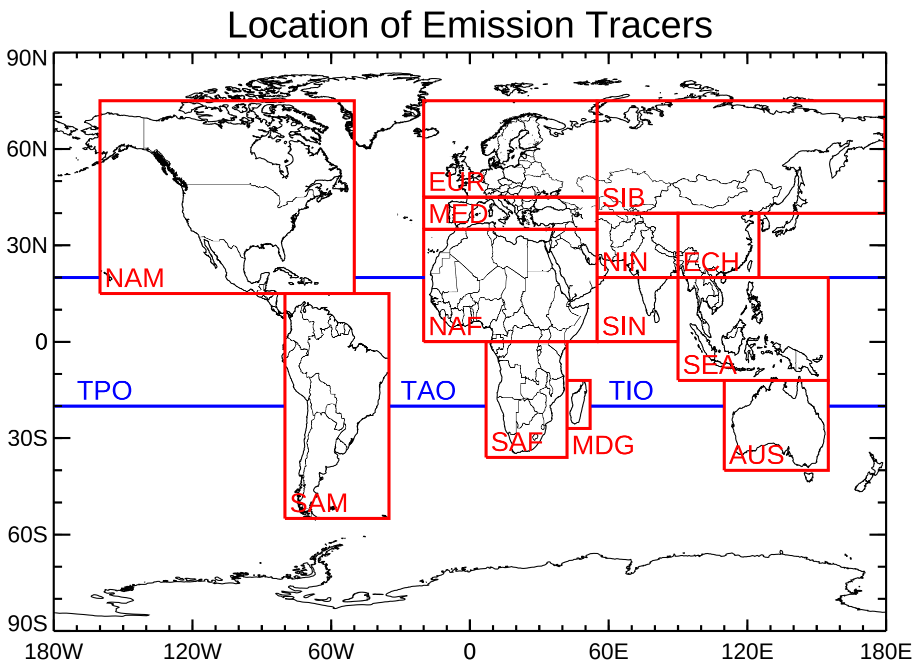

Figure 1. Global geographic location of artificial boundary layer source regions in the CLaMS model, also referred to as "emission tracers". The latitude and longitude range for each emission tracer is listed in Table 1.

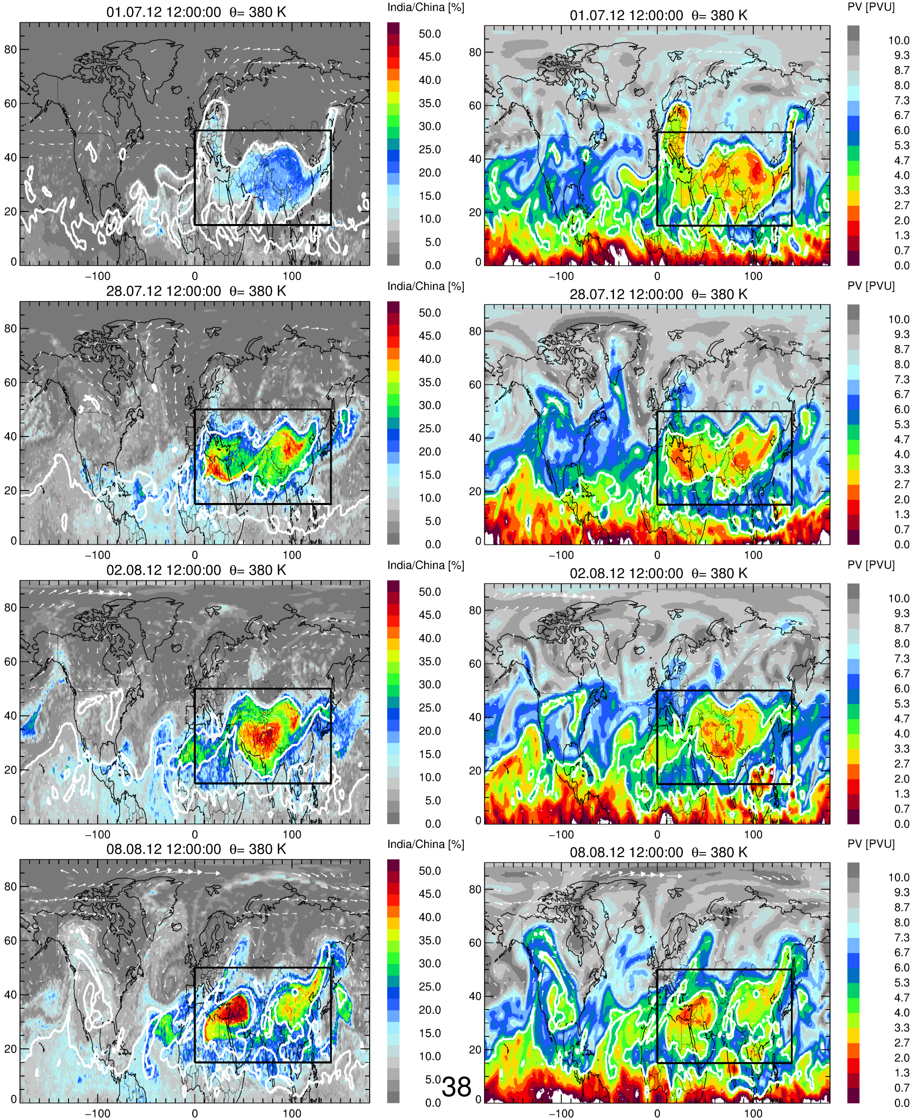
01.07.12 12:00:00 θ= 380 K
India/China [%]
PV [PVU]
28.07.12 12:00:00 θ= 380 K
02.08.12 12:00:00 θ= 380 K
08.08.12 12:00:00 θ= 380 K
50.0
45.0
40.0
35.0
30.0
25.0
20.0
15.0
10.0
5.0
0.0
10.0
9.3
8.7
8.0
7.3
6.7
6.0
5.3
4.7
4.0
3.3
2.7
2.0
1.3
0.7
0.0
80
60
40
20
0
−100
0
100

Figure 2. The horizontal distribution of the fraction of air originating in India/China (left) and PV (right) at 380 K potential temperature over Asia on 1 July 2012 (top), 28 July 2012 (2nd row), 2 August 2012 (3rd row), and 8 August 2012 (bottom). Please note that the order of the colour scale for India/China (left) and PV (right) is different, so that high contributions of emission tracers for India/China and low PV are marked in red. The horizontal winds are indicated by white arrows. The black rectangle (15–50° N, 0–140° E) highlights the region of the Asian monsoon anticyclone. The 4.5 PVU surface marks roughly the edge of the anticyclone shown as white thick line.

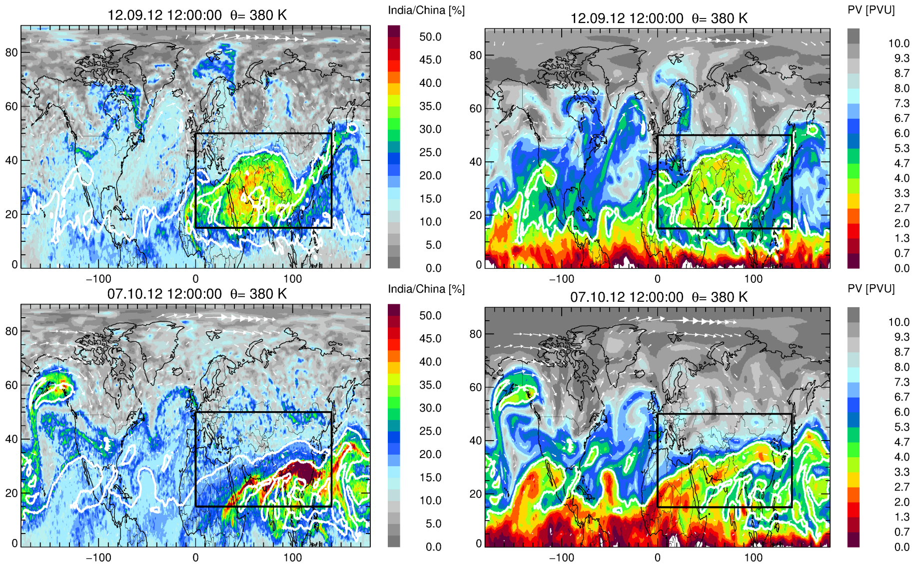

Figure 3. The same as Fig. 2, but on 12 September 2012 (top) during the late-phase of the anticyclone and on 7 October 2012 (bottom) showing the distribution of emission tracers for India/China after the breakup of the anticyclone.

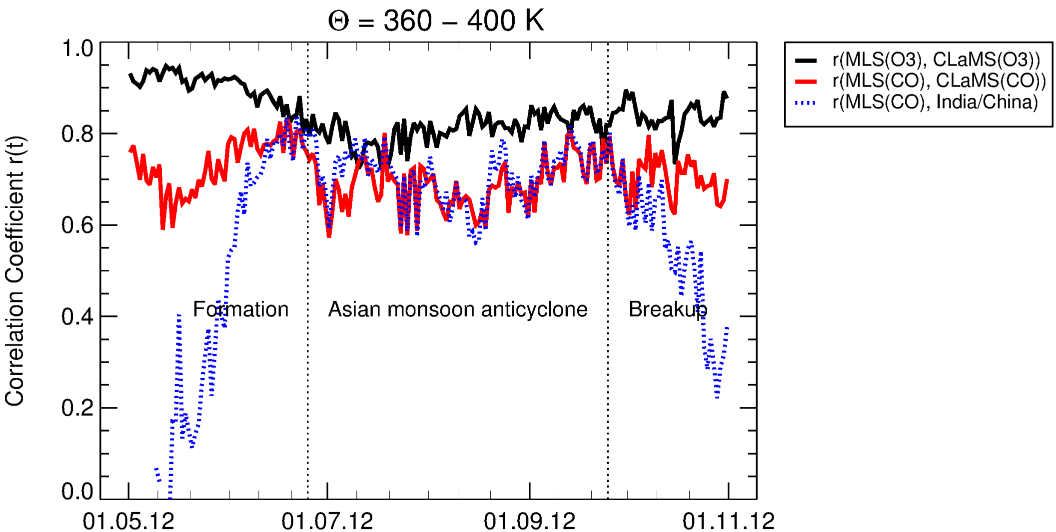

Figure 4. Correlation coefficients depending on time for tracer correlations patterns between MLS O_3 and CLaMS O_3 (black), between MLS CO and CLaMS CO (red), and between MLS CO and the CLaMS emission tracer for India/China (blue) for levels of potential temperature between 360 and 400 K (see text for more details) in a region between 15 and 50° N and 0 and 140° E (shown as black rectangle in Fig. 2 and 3).

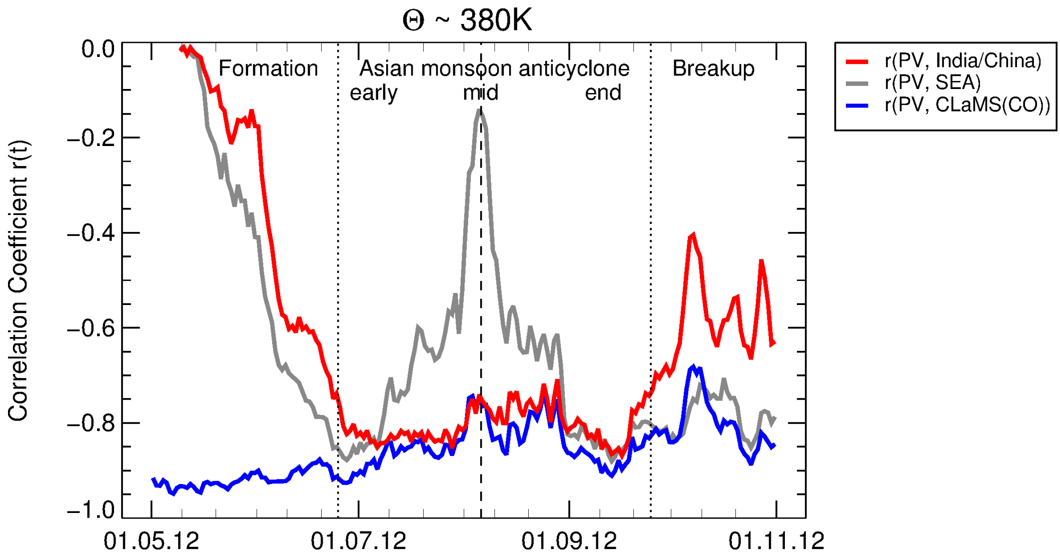

Figure 5. Time dependent correlation coefficients for the spatial distribution between PV and the emission tracer for India/China (red), the emission tracer for Southeast Asia (grey), and CLaMS CO (blue) at 380 K potential temperature (see text for more details) in a region between 15 and 50° N and 0 and 140° E (shown as black rectangle in Fig. 2 and 3).

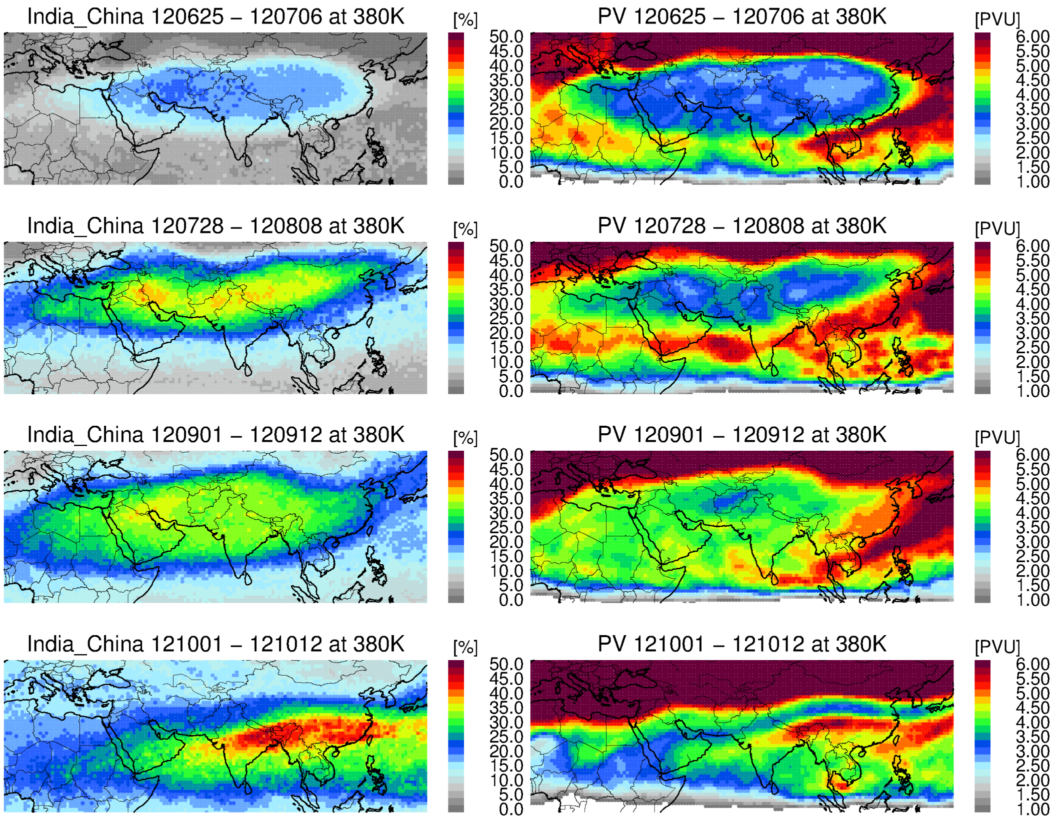

Figure 6. ~~Tweleve-day~~ Twelve-day mean values of the contribution of the emission tracer for India/China (left) and PV (right) during four different phases of the Asian monsoon anticyclone: early-phase (top) , mid-phase (2nd row), end-phase (3rd row) of the anticyclone and after the breakup (bottom).

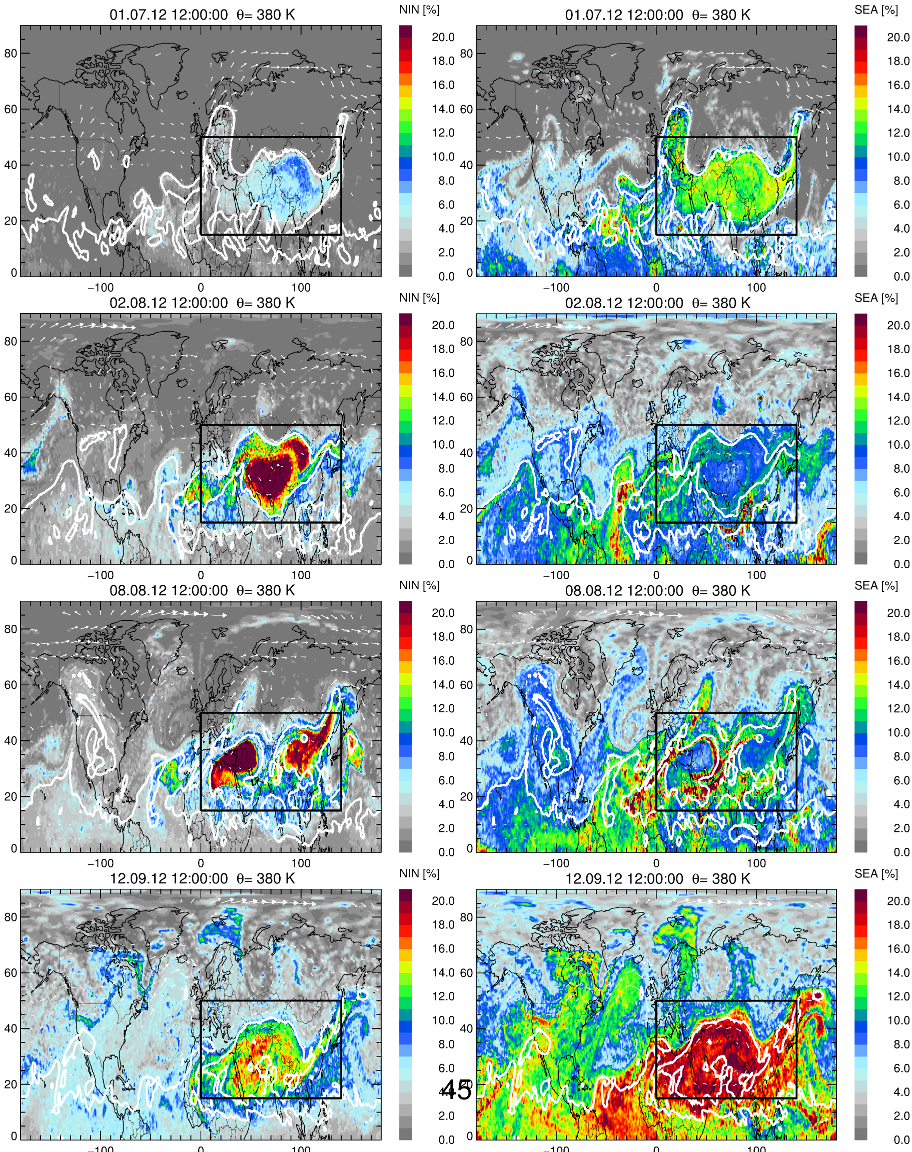
01.07.12 12:00:00 θ= 380 K
NIN [%]
01.07.12 12:00:00 θ= 380 K
SEA [%]
02.08.12 12:00:00 θ= 380 K
NIN [%]
02.08.12 12:00:00 θ= 380 K
SEA [%]
08.08.12 12:00:00 θ= 380 K
NIN [%]
08.08.12 12:00:00 θ= 380 K
SEA [%]
12.09.12 12:00:00 θ= 380 K
NIN [%]
12.09.12 12:00:00 θ= 380 K
SEA [%]
0.0 2.0 4.0 6.0 8.0 10.0 12.0 14.0 16.0 18.0 20.0
0 20 40 60 80
−100 0 100

The horizontal distribution of the fraction of air originating in (left) North India (NIN) and (right) Southeast Asia (SEA) at 380 K potential temperature over Asia on 1 July 2012 (top), on 2 August 2012 (2nd row), 8 August 2012 (3rd row) and 12 September 2012 (bottom). The horizontal winds are indicated by white arrows. The black rectangle (15–50° N, 0–140° E) highlights the region of the Asian monsoon anticyclone. The 4.5 PVU surface marks roughly the edge of the anticyclone shown as white thick line.

The horizontal distribution of the fraction of air originating in (left) North India (NIN) and (right) Southeast Asia (SEA) at 380 K potential temperature over Asia on 1 July 2012 (top), on 2 August 2012 (2nd row), 8 August 2012 (3rd row) and 12 September 2012 (bottom). The horizontal winds are indicated by white arrows. The black rectangle (15–50° N, 0–140° E) highlights the region of the Asian monsoon anticyclone. The 4.5 PVU surface marks roughly the edge of the anticyclone shown as white thick line.

Figure 7.
The horizontal distribution of the fraction of air originating in (left) North India (NIN) and (right) Southeast Asia (SEA) at 380 K potential temperature over Asia on 1 July 2012 (top), on 2 August 2012 (2nd row), 8 August 2012 (3rd row) and 12 September 2012 (bottom). The horizontal winds are indicated by white arrows. The black rectangle (15–50° N, 0–140° E) highlights the region of the Asian monsoon anticyclone. The 4.5 PVU surface marks roughly the edge of the anticyclone shown as white thick line.

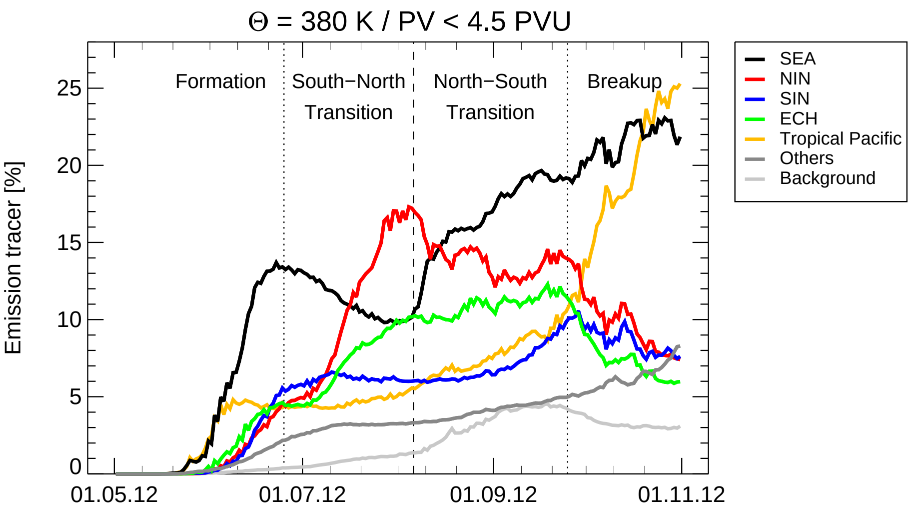

Figure 8. Temporal evolution of different emissions tracers from Southeast Asia (SEA, black), North India (NIN, red), South India (SIN, blue), East China (ECH, green), Tropic Pacific Ocean (yellow) and from all other land masses + Tropic Atlantic/Indian Ocean (others, dark grey) within the Asian monsoon anticyclone at 380 K from Mai 2012 until end of October 2012. Contributions of boundary sources not considered in the defined emissions tracers listed in Table 1 are summarised as background (light grey). The shown percentages are mean values calculated for air masses in Asia in the region between 15 and 50° N and 0 and 140° E at 380 ± 0.5 K (see black rectangle in Fig. 7) with PV values lower than 4.5 PVU that marks the edge of the anticyclone.

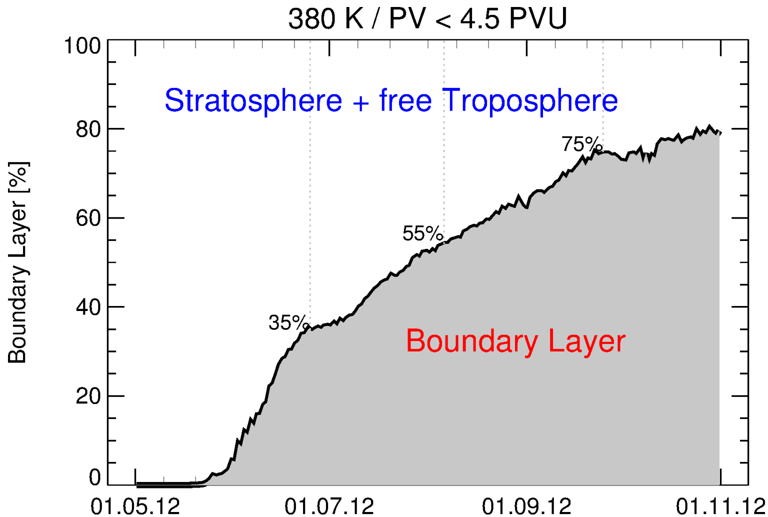

Figure 9. Temporal evolution of contributions of air masses from the boundary layer to the composition of the Asian monsoon anticyclone. The shown percentages are mean values calculated for air masses in Asia in the region between 15 and 50° N and 0 and 140° E at 380 ± 0.5 K (see black rectangle in Fig. 7) with PV values lower than 4.5 PVU that marks the edge of the anticyclone.